Journal of Advanced Research (2012) 3, 195–223

Cairo University

Journal of Advanced Research

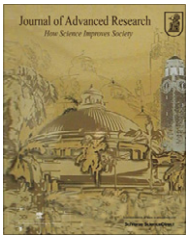

REVIEW ARTICLE

The synthesis, properties and uses of carbon materials with helical morphology

Ahmed Shaikjee [a,b], Neil J. Coville [a,b,*]

[a] DST/NRF Centre of Excellence in Strong Materials, University of the Witwatersrand, Johannesburg 2050, South Africa
[b] Molecular Sciences Institute, School of Chemistry, University of the Witwatersrand, Johannesburg 2050, South Africa

Received 6 April 2011; revised 21 May 2011; accepted 23 May 2011
Available online 3 August 2011

KEYWORDS
Coiled carbon nanotubes;
Coiled carbon nanofibers;
Carbon coil;
Carbon helix;
Synthesis;
Properties

Abstract Carbon nanostructures have been widely studied due to their unique properties and potential use in various applications. Of interest has been the study of carbonaceous material with helical morphologies, due to their unique chemical, mechanical, electrical and field emission properties. As such it is envisaged that these materials could be excellent candidates for incorporation in numerous nanotechnology applications. However in order to achieve these aspirations, an understanding of the growth mechanisms and synthetic strategies is necessary. Herein we consider historical and current investigations as reported in the literature, and provide a comprehensive outline of growth mechanisms, synthetic strategies and applications related to helical carbon nanomaterials.

Introduction

Carbon is an amazing element, not just because it is the element required for all life processes, but also due to the fact that it can exist in numerous allotropic forms [1]. Additionally, by means of synthetic processes, carbon can be tailored into a myriad of structures, particularly those in the nanometre range [2–4].

In 1991, Ijima published his landmark paper which described the appearance of carbon filaments with diameters in the range of nanometres [5,6]. These carbon materials would come to be known as carbon nanotubes (CNTs), and play a fundamental role in leading scientific and industrial research endeavours in nanotechnology. Indeed within a matter of years CNTs have taken centre stage in the nano-science arena. It is no exaggeration to say that one of the most active fields of research in the area of nanotechnology currently is the synthesis, characterization and application of CNTs [5,7,8]. This has naturally led to a renewed interest in the synthesis of other forms of carbon nanomaterials: graphene, fibers, horns, buds, onions, helices etc. [8–11]. It is this diversity in the morphology of carbon materials that provides the flexibility to modify the properties of carbon. Thus, the design and production of carbon materials with unusual morphologies is a promising way to exploit the morphology-property correlation of carbon nano-materials.

* Corresponding author. Tel.: +27 11 7176738; fax: +27 11 7176749.
E-mail address: Neil.Coville@wits.ac.za (N.J. Coville).

2090-1232

Peer review under responsibility of Cairo University.
doi:10.1016/j.jare.2011.05.007

Production and hosting by Elsevier

Of particular interest to scientists has been the study of carbon nanomaterials with a helical or non-linear morphology shown in Fig. 1. Helical carbon nano-materials have a long history, having first been reported by Davis et al. [12] in 1953. However these fibrous materials were initially considered a curiosity and efforts were focused on their prevention rather than on their synthesis [13,14]. It was not until the 1990s, stimulated by the discovery of CNTs, that there was a renewed interest in carbon fibers and tubes, especially those with unusual (e.g., helical/spring-like) morphology [2,3].

The helical shape is a common form seen in the universe (from spiralling galaxies to DNA) and it is thus not unexpected that this should also be a common motif found in carbon nanostructures [15]. Indeed innumerable macro-devices have been made based upon a helical design and used by humankind from ancient times (e.g., the Archimedes water screw) to the present (e.g., support springs for cellular keypads) [16]. It is expected that nano materials with helical morphology should possess both similar and unique physical and chemical properties to their macro components. Nano helices should thus behave in a comparable manner to macro materials with similar morphology. The ability of a macro scale spring to change shape in response to an external force (compression, extension, torsion etc.), and return to its original shape when the force is removed has made springs an important component in cellular technology, time keeping, medical as well as shock absorbing devices [16–18]. It is expected that the same should also apply to springs (helices) made from nanomaterials.

While mechanically useful, springs or coils have also been used in electro-magnets, solenoids, inducers etc. This is due to the ability of coiled materials to exhibit interesting electromagnet properties since a current flowing through a wire wound into a coil produces both electric and magnetic fields [16,18]. This property of electromagnetism has created a revolution in many fields from the development of plasma televisions to memory storage devices. It is envisaged that carbon nano-materials with helical morphology could also be used as components in future nano-technology devices [13,19,20].

Macro sized coils and springs are manufactured by a top down process. While this approach could also be used to form nano sized springs, the bottom up process starting from atoms and molecules is expected to be the preferred procedure to make the components needed to form helical nano-materials. The growth of helical carbonaceous materials from carbon precursors via a bottom up approach in the presence of a catalyst is expected to proceed by equivalent methods used to synthesize straight fibers and tubes [5,7]. The mechanism commonly proposed for carbon fiber growth involves adsorption and dissociation of a carbon precursor on the surface of a catalyst particle and dissolution of carbon into the catalyst particle. Once the catalyst particle has been saturated with carbon, the carbon crystallizes out of the metal particle and is extruded to form a

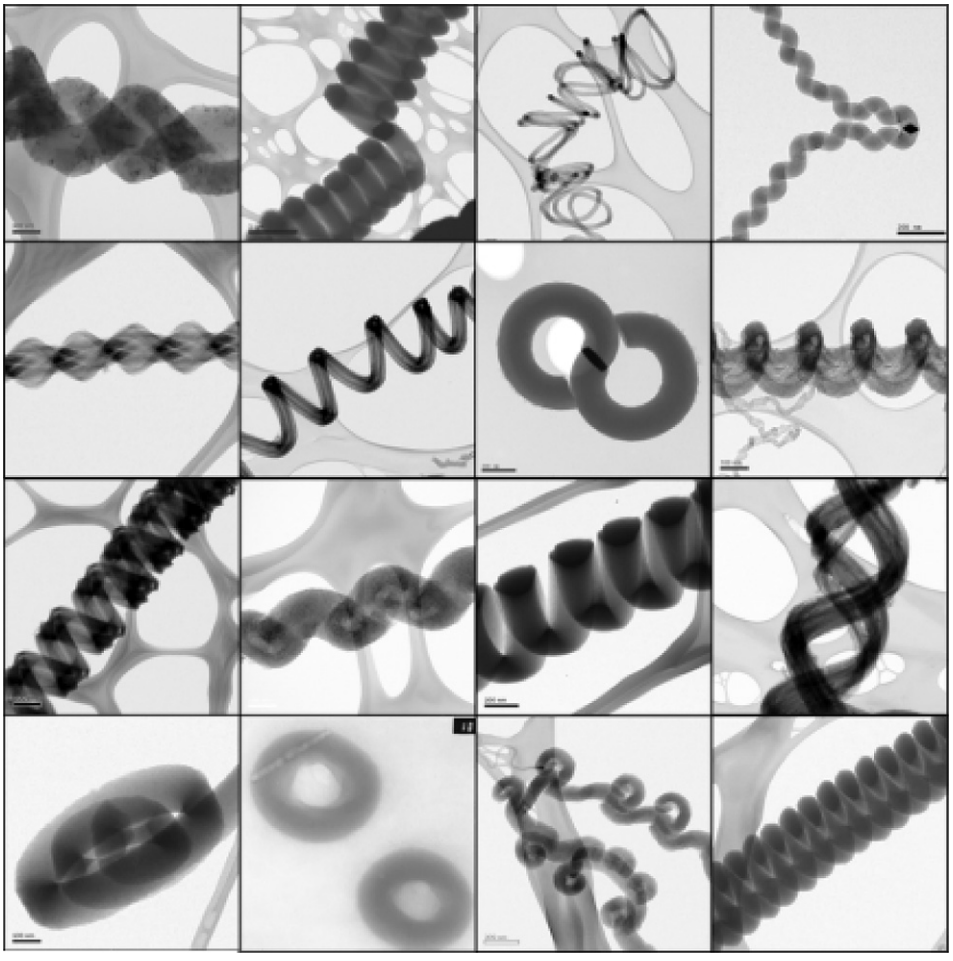

Fig. 1 Various types of helical carbon nanomaterials with non-linear morphology.

CNT or CNF [5,20]. Typically CNTs exist as cylinder/s of rolled up graphene sheets [7], giving rise to single walled, double walled and multi-walled entities, Fig. 2. CNFs by contrast are composed of graphene sheets that stack upon each other, to produce both hollow and solid carbon structures, Fig. 2. These structures do not need to be straight; they can take on a helical morphology. As such, two categories of helical materials exist; (i) coiled fibers, Fig. 3a, where the fiber is a dense structure with no inner hollow and (ii) coiled tubes, Fig. 3b, where an inner hollow exists throughout the length of the coil.

Helical carbon fibers and tubes can be divided into different categories based upon the helical nature of the material: single helix, double helix, triple helix, braid, spiral, coil, spring etc. [3,15,19]. The diversity of helical materials provides a myriad of shaped carbons, Fig. 1. The use of helical carbons in technological applications will be dependent on our ability to control the coil morphology and coil geometry of these materials. This includes control of the coil diameter, pitch and fiber/tube thickness, Fig. 3c. The growth of carbon nano-materials can be controlled by varying temperature, gas environment and the type of catalyst. The alteration of any of these variables will result in a significant change in the type and amount of helical carbon nano-materials formed [3]. To achieve this control, an understanding of the growth mechanism and the role played by the various parameters is needed. To date control over the synthesis of a specific type of helical carbon nano-material has been met with only limited success.

In this review we attempt to provide a summary of the various synthetic procedures employed, the relevant mechanistic explanations that have been given to explain helical growth patterns and the current technological applications associated with the new generation of helical carbon nano-materials that have been prepared. In so doing we provide a way forward for controlling the synthesis of helical carbon materials and hence the manufacture of sophisticated and economically viable nano-devices containing carbon nano helices.

Structural origin and growth aspects of carbon helices

After the discovery of CNTs, researchers began to study other forms of carbon in greater detail; in particular those that exhibited non-linear geometry. The use of a graphene sheet or honeycomb network rolled into a cylinder (used to model CNTs) could not be used to explain the geometry observed in non-linear carbon structures. In early studies it was realised that fullerenes achieved their curvature by the introduction of pentagonal rings into graphene (positive curvature) while the insertion of heptagonal and/or octagonal rings led to 'negative' curvature [21,22]. Before long it was appreciated that a judicious insertion of a series of pentagonal and heptagonal rings within a hexagonal matrix would yield helically coiled carbon nano-materials. As such the issue of helical growth is then to achieve the correct combination of polygonal rings (5, 6 and 7) that would generate a helix [22–25].

Structural origin of helices in CNTs

In order to develop a model that can describe the helical nature of coiled CNTs, carbon in the form of a fullerene or torus must first be considered. Dunlap [21,26] showed that the insertion of pentagon and heptagon rings at the junction of two CNTs can yield what he called a 'knee structure'. A knee is formed by the presence of a pentagon on the convex (positive curvature) side and of a heptagon on the concave (negative curvature) side of

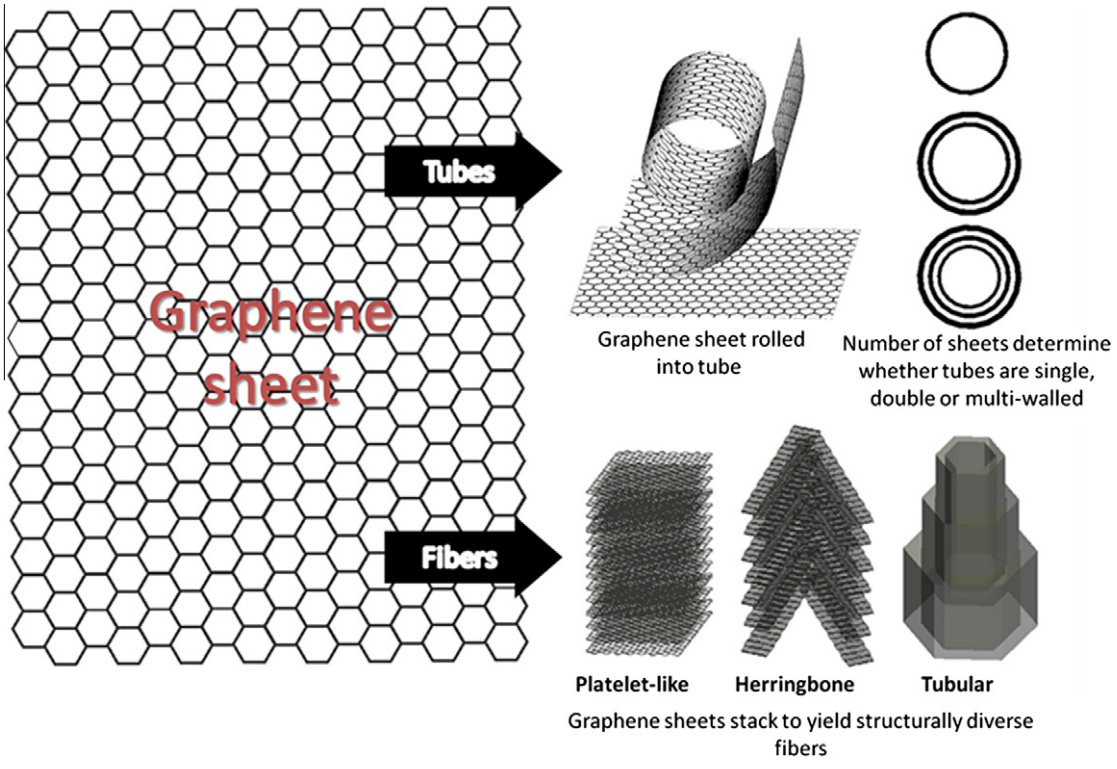

Fig. 2 Arrangement of graphene sheets to produce carbon nanotubes and fibers with various morphologies.

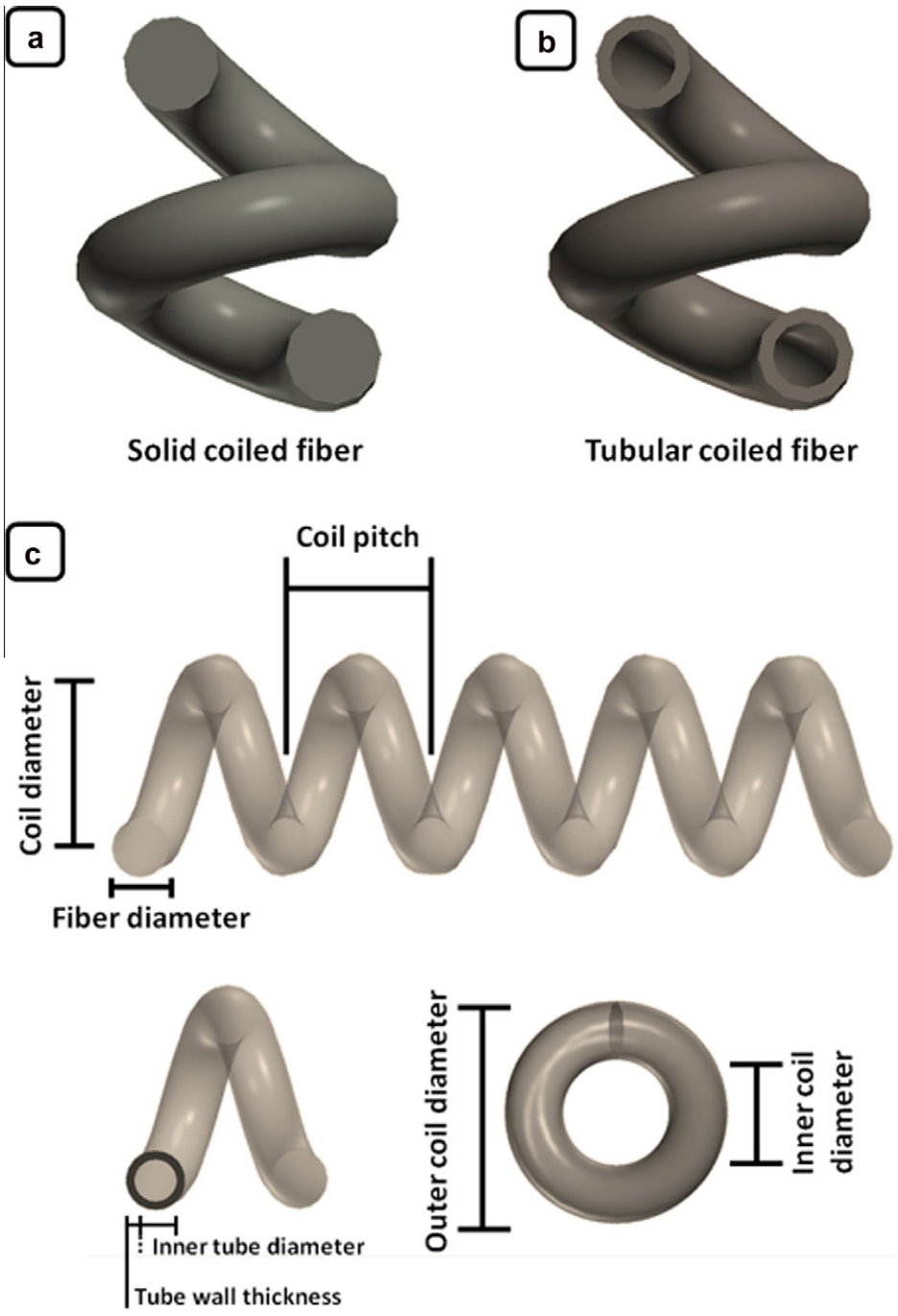

Fig. 3 Schematic illustration: (a) solid coiled fiber, (b) tubular coiled fiber and (c) parameters used to define coil morphology.

a graphene plane, Fig. 4. The concept of carbon nanotube 'knees' proposed by Dunlap was extended by Fonseca et al. [24] who showed that knee segments could be joined together to form a toroidal structure (containing 520 carbon atoms, 10 knees). Additionally they were also able to show that if the knees are joined in such a way that consecutive knees are joined out of plane, a helix or coil will form instead of a torus.

Ihara and Itoh [22] showed that structures that included pentagons and heptagons gave a variety of toroidal structures that were thermodynamically and energetically stable, Fig. 5. They were able to show that toroidal carbon structures could be used to model helical CNTs. It was noted that the type of toroidal segment used determines the coil pitch, diameter and cycle of the helix, Fig. 5b (C_{360}) and Fig. 5c (C_{540}). Additionally they concluded that the arrangement of heptagons within the carbon matrix was instrumental in controlling the coil geometry. A study by Setton and Setton [27] concluded that while toroidal segments could be used to model helical CNTs, they could only be used to explain single shell helices or at best two shell helices. They suggested that for multi shelled helices, pentagon and heptagon pairs would have to be arranged along the helical path, or alternatively other 'defects' would need to be considered. Most recently Liu et al. [28] were able to demonstrate, using atomistic models, that by introducing a pair of pentagons and a pair of

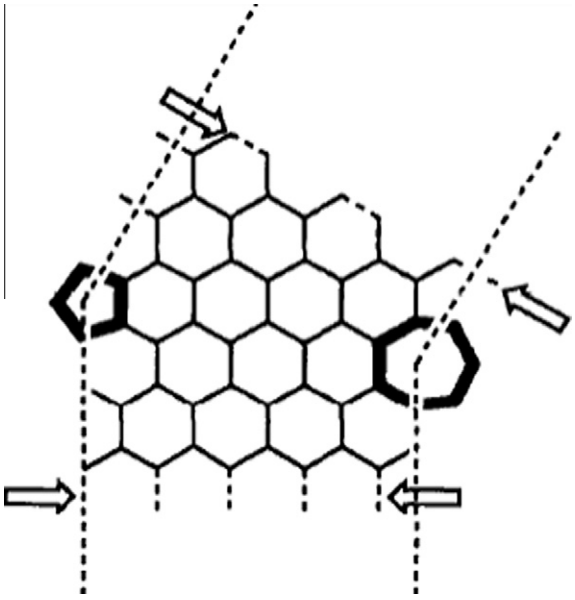

Fig. 4 Knee formed by pentagon/heptagon pair [24].

heptagons into the structure of a single walled CNT that a curved structure could be obtained. The pair of pentagons forms a cone defect whereas the pair of heptagons results in a saddle point. The incorporation of the pentagons/heptagons creates strain, which is released when the CNT bends at the defect site. They suggested that by varying the diameter of the nanotube and/or the length of the basic segment, the coil diameter, coil pitch and tubular diameter could be varied. Biró et al. [25] attempted to explain the incorporation of pentagon/heptagon pairs by considering the possibility that pentagon/heptagon pairs were not simply defects but were regular building blocks for the helical CNT structure. They proposed that Haeckelite type sheets, which are characterized by a high number of pentagon/heptagon pairs, could be rolled like a graphene sheet to yield helical CNTs, Fig. 6. Furthermore experimental observations of Haeckelite type structures indicated that they could be produced by procedures analogous to those used to generate CNTs. Lu et al. [29] proposed that during the initial growth of helical CNTs, prevailing reaction conditions would result in the nucleation of a pentagon, which would result in the formation of a spiral shell around a catalyst particle, Fig. 7 [19]. From

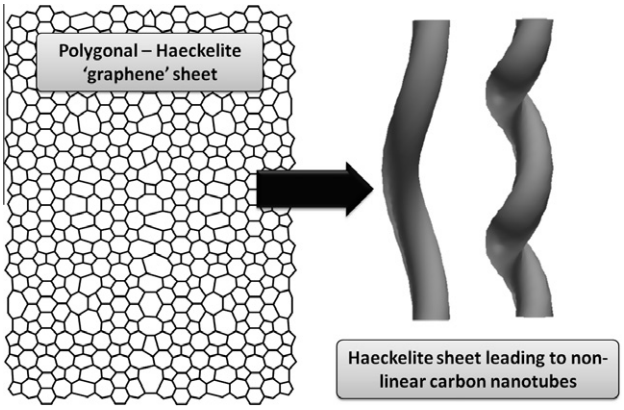

Fig. 6 Haeckelite structure, graphite sheet composed of polygonal rings, that can be rolled to form helical nanotubes (based on ref [25]).

this core structure, curved or straight segments emerge that depend upon whether there are only hexagons (straight segment) or pentagon/heptagon pairs (curved segments) present. As such, geometric parameters (coil pitch, twist angle etc.) are determined by the frequency of pentagon/heptagon pair creation. While these models are useful, they cannot explain how pentagon/heptagon pairs can be incorporated in such a manner.

Fonseca et al. [24] attempted to explain the introduction of 'knees' (pentagon/heptagon pairs) by means of steric hindrance. They proposed that if the growth path of a CNT was blocked, formation of a knee at the catalyst surface would cause a bend in the tube before continued growth, Fig. 8. As further blockages were encountered further knees would be introduced, resulting in regular and irregular helically coiled CNTs. However this model has been met with limited acceptance as blockages would have to be systematic (to ensure regular coiling) and adjacent tubes would be expected to interfere with each other's helicity as they collided during growth.

While the concept of pentagon/heptagon pairs has been accepted as the best model to explain helical growth, Ramachandran and Sathyamurthy [30] have suggested that rotational distortion of carbon fragments, that do not alter the hexagonal matrix is also capable of yielding helical CNTs. They suggested that as a CNT grows, the adjacent layers can undergo rotational distortion by some small angle from their original position. This continued distortion of subsequent layers results

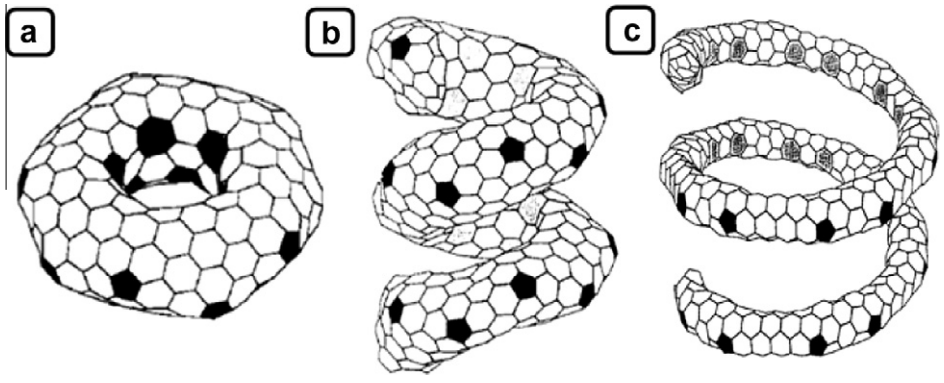

Fig. 5 (a) Toroidal structure made up of pentagons and heptagons (C_{360}), (b) helical coil made up of toroidal (C_{360} segments), (c) helical coil made up of toroidal (C_{540} segments) [22].

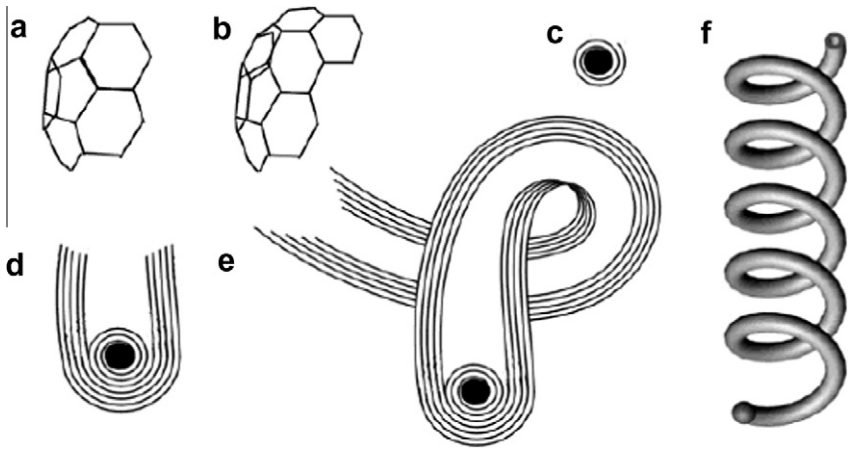

Fig. 7 Growth model for helical CNTs: (a–c) development of isocahedral shell, (d) growth of straight segment followed by, (e) helical segment as pentagon/heptagon pairs are introduced into the growing matrix, (f) formation of coiled CNT [19].

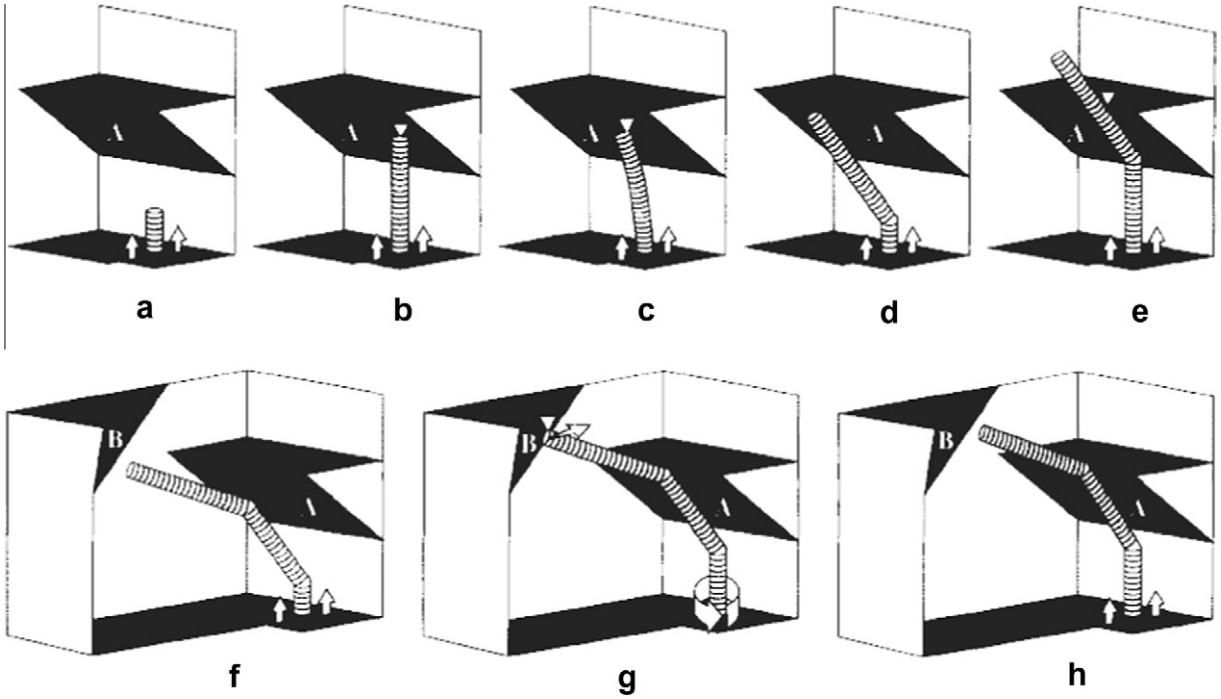

Fig. 8 As a growing nanotube encounters an obstacle it changes direction (bends) so as to continue growth. Bends are thought to occur by introduction of pentagon/heptagon pairs [24].

in a coiled nanotube. This mechanism eliminates the need for incorporation of pentagon/heptagon pairs, as the hexagonal matrix is maintained albeit in a distorted geometry.

Structural origin of helicity in CNFs

While the helicity of CNTs has been modelled around the inclusion of pentagon/heptagon pairs into a hexagonal framework, this approach cannot be used to fully explain helicity in CNFs. Helical carbon fibers range from the amorphous to highly crystalline, and vary from nanometre to micrometre sizes. Attempts to relate helicity to the molecular structure of CNFs via a graphene sheet (whether curved or not), have been made. Typically, the helical nature of carbon fibers is thought to be caused by the unequal extrusion of carbon from a catalyst surface and this effect gives rise to the curvature, Fig. 9 [31]. As such, external stresses and catalyst composition should then impact directly on the helical nature of carbon fibers. An alternative suggestion has been made by Zhang et al. [32] who proposed that helical carbon fibers form from catalyst particles that are influenced by van der Waals forces that exist between the fiber and surroundings. As these forces change with temperature, unequal extrusion coupled with other stresses will lead to curvature of the fiber and ultimately helicity, Fig. 10.

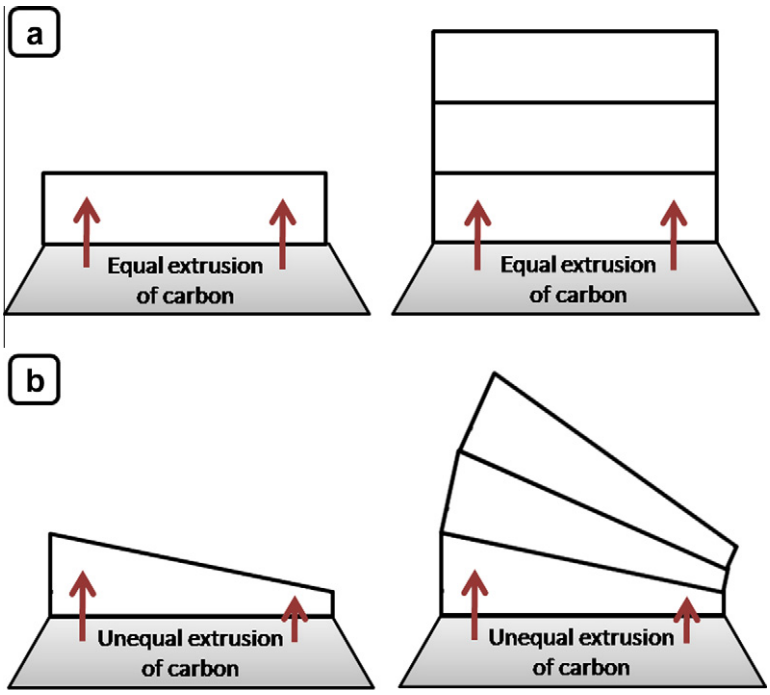

Fig. 9 (a) Equal extrusion of carbon to yield straight fiber, (b) unequal extrusion resulting in non-linear fiber.

From the above it is apparent that the structural origin of helical carbon nano-materials still requires investigation as current models, while useful, do not fully explain the diverse range or periodicity of helical structures, and most importantly how or why pentagon/heptagon pairs form.

Growth aspects of carbon helices

Most researchers have considered the insertion of pentagon/heptagon rings within the hexagonal lattice of a tube, or the unequal extrusion of carbon from a catalyst particle to explain the origin of coiling or helicity of carbon nanomaterials [24,25,31]. However, the means by which these phenomena may be interlinked is not yet fully understood. To date most efforts have focused on the effect that catalyst morphology and composition have on the evolution of helical carbon materials, with some interest dedicated to the effect of other external factors.

Effect of catalyst/graphite interfacial interactions

Various mechanisms have been proposed to explain the development of non-linear or helical carbon nanostructures. Amongst the ideas currently entertained, one proposal is that growth occurs due to the presence of wetting/non-wetting catalyst particles that promote linear or non-linear growth respectively [33,34]. A second proposal is that growth occurs from bimetallic catalysts that operate using cooperative means [16].

Bandaru et al. [33] proposed that nanocoils are formed only by the use of certain catalysts or substrates. They considered the interfacial tension that exists between the metal catalyst particle and graphite surfaces. This interfacial tension, known as wettabillity, is used as a criterion for coiling. Liquid metals

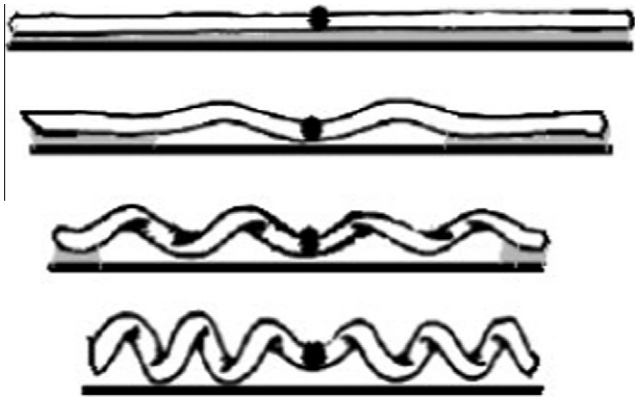

Fig. 10 As van der Waals interaction changes (grey area), straight fiber twists to form a coil [32].

such as In, Cu and Sn, which are known to induce helicity have large wetting angles ($>150°$), whereas Ni, Fe and Co which predominantly produce linear carbon materials have smaller wetting angles ($<75°$). Small wetting angles result in a net attractive interaction with the growing carbon surface resulting in linear growth, while large wetting angles result in repulsive interaction that promotes non-linear growth (non-wetting). Bandaru et al. explained this concept by considering an In/Fe catalyst, where Fe was thought to act as the growth point, and In as the promoter for helicity. They observed that as the In content was increased, tighter coils (small coil pitch) could be formed, whereas lower In content yielded coils with larger pitches. A higher In content, results in a greater number of In particles that are available to interact with the carbon structure, thereby inducing a greater number of bends, and vice versa, Fig. 11a. From their analysis they proposed that In

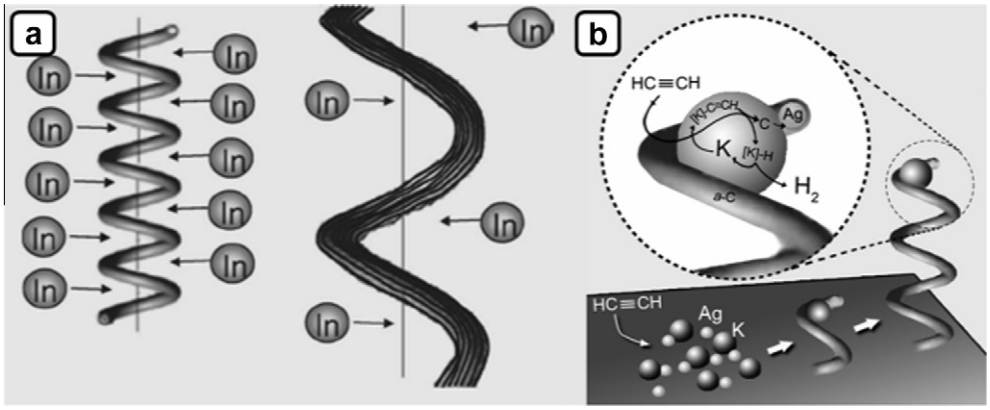

Fig. 11 (a) Non-wetting catalyst particle (In) causes non-linear deformation; as the concentration of the catalyst decreases coil tightness decreases [33]. (b) Co-operative wetting catalyst particle (K provides a template onto which growing carbon coils can form) [34].

particles are indirectly responsible for coiling and can be considered as an external stress.

Liu et al. [34] described the use of a K/Ag catalyst to form helical carbon fibers. They observed that individually neither K nor Ag could yield coiled carbon fibers, but that both acted co-operatively to decompose acetylene and promote growth. It was proposed that the Ag particle acts as the seed for fiber growth and that K, in addition to decomposing acetylene, acted as a template to facilitate coil formation. Liu et al. suggested that the growing fiber curls along the carbon–K interface, Fig. 11b, a phenomenon attributed to the wetting capability of K (liquid K can wet carbon effectively).

The proposals made by Bandaru et al. and Liu et al., considered the interfacial interactions of catalyst and carbon nano-material in two different ways. While they may seem contradictory it must be noted that Bandaru et al. considered the non-wetting catalyst particle (In) to be indirectly responsible, acting as only an external stress. However Liu et al. suggested that K played an active and direct role in coil formation, providing a template onto which the growing carbon fiber can be formed. The different growth mechanisms, illustrate the complexity involved in understanding the formation of helical carbon materials.

Effect of catalyst morphology

To date researchers have placed a great deal of emphasis on the relationship between the nature of the catalyst used and the type of carbon nanostructure produced [3,5]. It has been observed that the growth point for helical carbon nanomaterials is associated with a catalyst grain. Apart from the composition of the catalyst used, two main issues have been identified: (i) the relationship between the size of the catalyst particle and the type of carbon associated with it and (ii) the regularly faceted shape associated with these catalyst particles.

Researchers have frequently suggested that the selective growth of helical carbon materials can be achieved by the careful control of the catalyst particle size. Zhang et al. [35] observed that for carbon nanofibers grown from nano Cu catalysts at 250 °C, coiled carbon fibers were obtained when catalyst particles were between 30 and 60 nm in diameter. However, only straight carbon fibers were obtained when catalyst particles were >120 nm. Hokushin et al. [36] showed that for carbon nanocoils grown from an Fe/In/Sn catalyst at 700 °C, particles larger than 200 nm were not active for the growth of carbon nanocoils (CNCs). CNCs were only observed in large quantity for particle sizes ranging between 50 and 150 nm. The effect of particle size was further evidenced by Tang et al. [37], who observed that for an Fe_2O_3 catalyst, helical carbon nanomaterials with good helical structure grew from catalyst particles with diameters < 150 nm. As the size of the catalyst particle increased (150–200 nm) the helical structure was compromised by the appearance of straight segments. At diameters above 250 nm only straight CNT bundles were observed. Similar observations have been made by other researchers leading many to conclude that catalyst particle size was the determining factor in controlling carbon fiber helicity [3,38,39]. However particle size cannot be the only factor, as it does not explain the wide range of carbon nano/micro-coil morphologies that have been synthesized, or how size relates to helicity [3,11,40]. As such, in conjunction with size, one must consider the shape of the catalyst particle as well.

Dating back to the early 1990s, Motojima et al. [41] and Kawaguchi et al. [42] reported that diamond shaped catalyst particles were associated with the appearance of carbon micro-coils (CMCs), Fig. 12a. These observations were further highlighted by numerous other researchers who reported on the presence of regular and well faceted particles associated with other forms of helical carbon materials, Fig. 12b [11,19,43–47]. These faceted particles provided for a plausible mechanism by which carbon could achieve helical growth. It was postulated that the faceted particles could provide surfaces (faces) with variable extrusion characteristics that would lead to unequal carbon extrusion rates and curvature of the extruded carbon fiber [43,47,14,48]. This concept of variable extrusion based upon different facets of a catalyst particle has gathered support over time and is among the leading ideas currently proposed to explain the appearance of helicity. Xia et al. [49] were able to demonstrate that carbon nanohelices grown from an Fe_3C catalyst particle, had catalyst particles that were hexahedra, i.e., made up of six different crystallographic planes, Fig. 13. They concluded that the different crystallographic surfaces produce an anisotropic growth that caused the particle to rotate as the fiber grew, thereby introducing helicity. Li et al. [50] showed that the geometric structure of the catalyst particle affected the type of carbon extruded. They also suggested that these catalyst particles were made up of hexahedra that contained two types of crystal facets, those with, and those without carbon precipitation (extrusion).

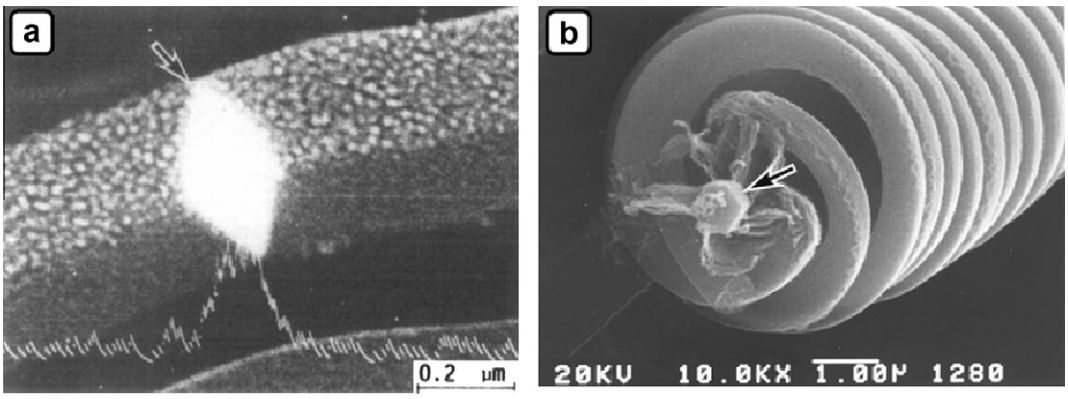

Fig. 12 (a) Diamond shaped catalyst particles as reported by Motojima et al. [41] (b) and faceted hexahedral particle as reported by Chen et al. [43].

As the number of precipitation facets increased from two to three, there was a corresponding change from a double to a triple type of helix. Furthermore Li et al. [50] suggested that the bulk diffusion of carbon to the other facets was anisotropic and it was this anisotropic diffusion that led to curvature of the extruded fiber and formation of helices.

However it has been observed by Qin et al. [51] that regular faceted particles do not necessarily yield helical carbon materials. They showed that Cu catalyst particles associated with straight fibers were also regular and faceted, Figs. 14a and b, albeit with a larger particle size than those associated with helical fibers. As such, further examination of these particles is necessary. Recently we have reported on the relationship between catalyst particle morphology and corresponding fiber morphology [52]. It was observed by TEM tilting procedures that a 3D model of the catalyst particles could be produced, and that the shapes of catalyst particles that produced different helical morphologies were different. As the number of facets changed from 4 to 6, there was a corresponding change from a Fibonacci-like to a spiralled helix, Fig. 15. The morphology of the catalyst particle thus impacts on the type of carbon fiber extruded. Size and shape are thus not mutually exclusive in determining carbon helicity

Templates and other external stresses

While the exact mechanism by which helical carbon materials form still remains unclear, researchers have been able to show that external stresses can be manipulated into assisting with the formation of non-linear structures, regardless of the composition or morphology of the catalyst particle. In-Hwang et al. [53] attempted to influence the growth of CMCs by utilising a rotating substrate. They observed that when the catalyst substrate was rotated there was a gradual loss of regular coiling with increased rotation speed, Figs. 16a–c. AuBuchon et al. [54] were able to show that a change in the direction of an applied electric field during carbon fiber growth was capable of altering the fiber morphology, Figs. 16d–e. As such they were able to synthesize CNTs with a non-linear zigzag morphology. Joselevich [55] described the growth of carbon serpentines by the surface directed growth of carbon nanotubes. By utilising patterned templates (SiO_2 with atomic steps) and directed flow rates, CNTs were shown to grow and conform to the shaped nanosteps; as such serpentines and other non-linear CNT's were produced, Fig. 16f. Akagi et al. [56,57] considered the growth of helical polyacetylene (thin films) by using chiral agents, soft templates and applied magnetic fields. While these polyacetylenes are considered as polymers, they are composed in some instances of carbon fibrils that are less than 100 nm in diameter. The methodology highlights an alternative route to make carbon materials with helical morphology. These methods illustrate that while catalyst composition and morphology play a dominant role in controlling fiber morphology, growth can be altered by introducing certain external stresses.

Synthesis of helical carbon materials

Ever since they were first observed, researchers have generated a diverse range of synthetic conditions and reactions that are capable of producing helical carbon materials. While the different approaches used have benefits and drawbacks, the most promising method appears to be the catalytic chemical vapour deposition (CCVD) method. In the CCVD approach, reaction parameters can accurately be controlled [3]. CCVD allows for the use of a wide variety of liquid, solid or gaseous carbon sources as well as a variety of reactor designs to be employed. Additionally helical carbon materials are observed to form under a wide range of temperatures and pressures, and in the presence of numerous reactive agents and catalysts. These studies, listed in Tables 1 and 2, have revealed that typical requirements necessary to form helical carbon materials include: (i) impurity elements such as P, S (ii) promoter metals such as Cu, Sn, In and (iii) catalysts such as Ni, Fe, Co for the growth of the carbon material and (iv) and an appropriate carbon source [3,11,58].

A summary of publications that have described the synthesis of helical CNTs and CNFs are listed in Tables 1 and 2 respectively [34,36,37,40,41,43,45,47,14,50,53–93,32]. It can be concluded that helical materials obtained in high yield and selectivity, Fig. 17, are obtained by using catalysts composed of Fe, Ni or Cu, with additives or impurity elements such as Sn and S. Based upon the type of catalyst used and temperature employed, selectivity of helical, twisted

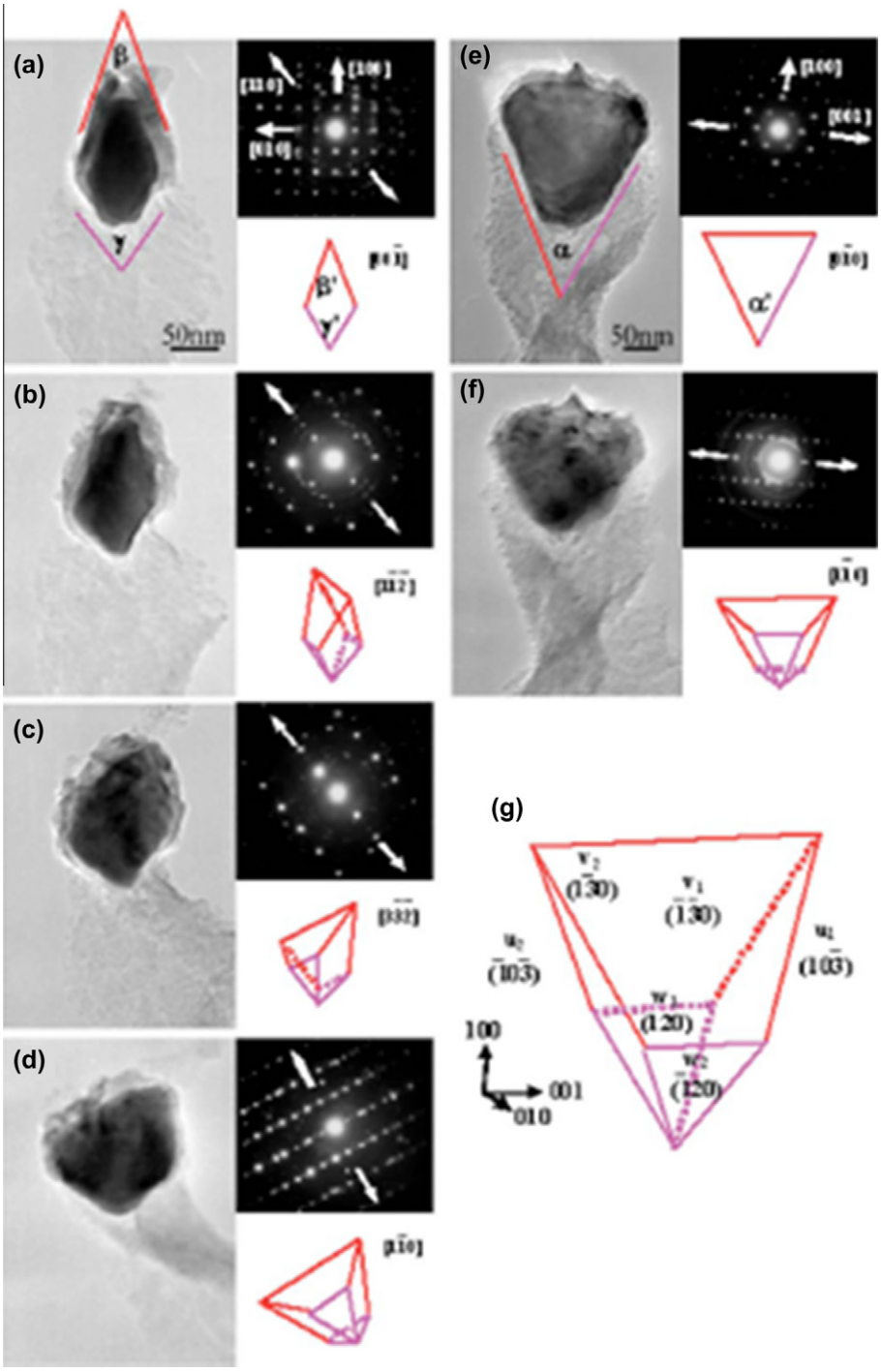

Fig. 13 Hexahedral catalyst particle at different angles, showing facts with different crystallographic indexes [49].

or intertwined carbon tubes/fibers can be manipulated by a range of parameters. It is also observed, that in almost every instance that the carbon source (precursor) used to form helical CNTs, is acetylene. Currently there are limited reports on the synthesis of single or multiwalled CNTs (highly ordered) with helical morphology. However greater success has been achieved in making crystalline and amorphous helical carbon fibers. Interestingly it is clear that there exists no system that distinctly relates catalyst type with carbon morphology.

Properties and applications

CNFs with spring-like morphology are of great interest due to their unique 3D morphology. Researchers have often envisaged these materials as having the potential to be incorporated in various nano-technology devices as mechanical components in the form of resonating elements or nano-springs and in novel reinforcement composites [3,11,19,94]. However, before these materials can be fully utilized their physical, chemical

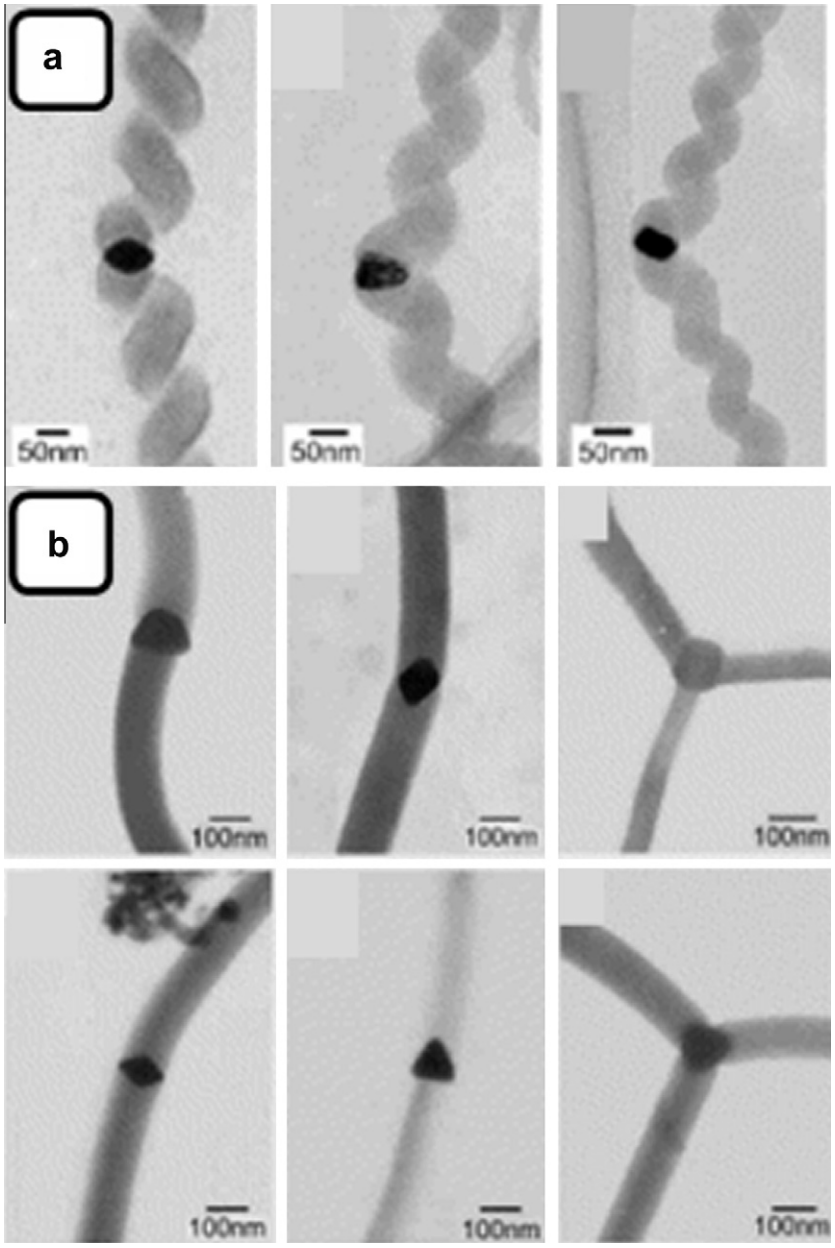

Fig. 14 Regular faceted particles giving rise to (a) helical nanofibers, (b) linear nanofibers [51].

and mechanical properties need to be examined and understood. Much like a spring, factors such as elongation under strain, changes in coil diameter and pitch, spring constants (the ratio of the force affecting the spring to the displacement caused by it) as well as Young (the ratio of stress to strain, linear strain) and shear (the ratio of shear stress to the shear strain) moduli need to be measured and calculated [16,95]. Additionally the resistivity, conductance, electro-magnetic and electro-mechanical capabilities of helical carbon materials also need to be understood and fine tuned [18].

Mechanical behaviour

Motojima et al. [41] were amongst the first (1991) to investigate the extension characteristics of CMCs. They reported that carbon micro-coils with a diameter of 0.5 μm and a coil pitch of 5 μm could be extended up to 3 times their original length, without deformation upon release. However upon extension to 4.5 times (almost linear) the coils did not recover to their original geometry. These observations were later confirmed by Chen et al. [96] who showed that carbon micro-coils that were extended to 3.5 times their length could retain their morphology once the extension force was released. Again, CMCs that were extended to an almost linear state did not retain their original geometry. In order to provide additional physical characteristics such as elastic spring constants and the Young's modulus for the carbon coils (grown over an iron and indium tin oxide catalyst at 700 °C using C_2H_2), Hayashida et al. [97] attached the edge of a single coil to the tip of Si cantilever. The CNCs (tubular) was then manipulated by moving the Si tip. It was found that these tubular CNCs (double intertwined) could

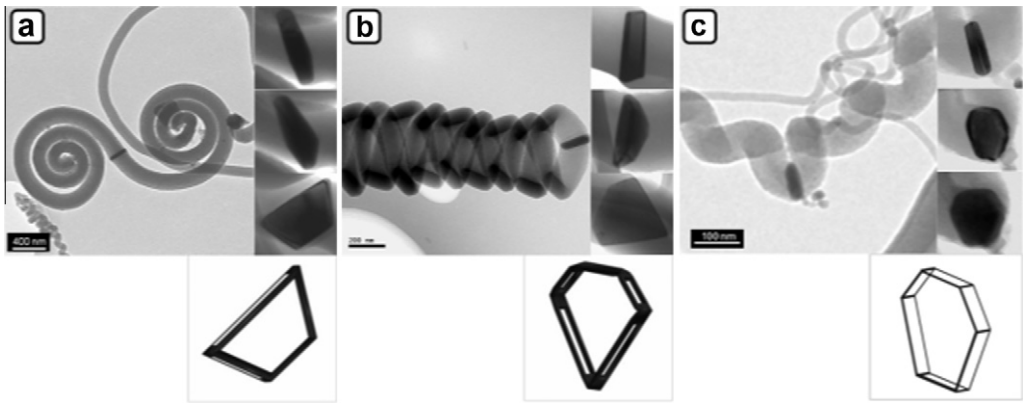

Fig. 15 Morphology of catalyts particles associated with fiber morphology: (a) trapezoid giving rise to Fibonacci spiral, (b) planar pentagon associated with double helix, (c) planar hexagon associated with helical fiber [52].

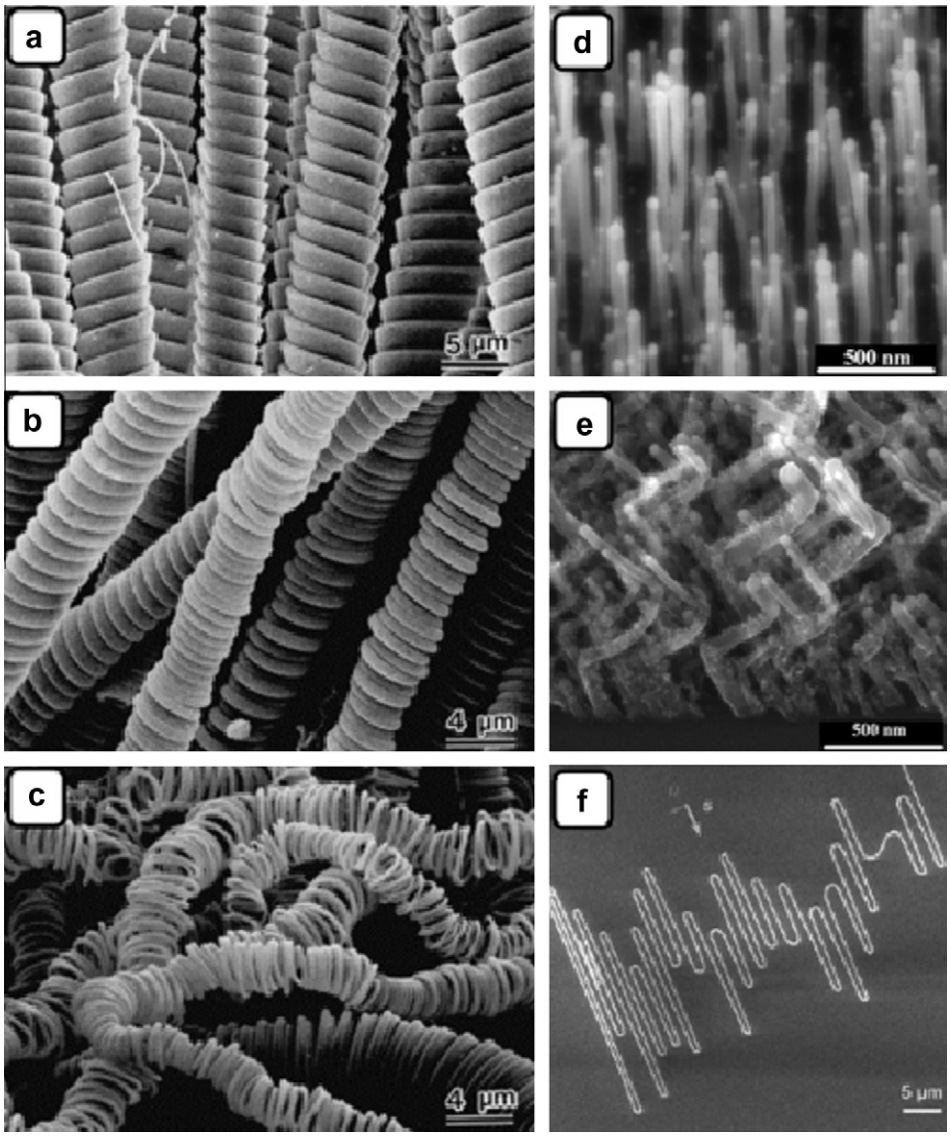

Fig. 16 Types of non-linear carbon materials produced by external stresses: (a–c) rotation of substrate, with increasing speed [53], (d and e) change in current direction, straight fibers becoming zigzag [54], (f) nanosteps of crystal surface leading to serpentine structure [55].

Table 1 Synthetic parameters related to the synthesis of helical carbon nanotubes.

Reference	Tubes/tubules				
	Type of carbon	Catalyst	Gas atmosphere	Temperature (°C)	Reactor
Qi et al. [59]	Helical carbon nanotubes, with V, Y and V/Y shaped structures (double or triple coiled carbon nanotubes) connected to a single catalyst particle. Tube diameters of 30–70 nm and coil pitch and diameters of 50–100 nm	Fe catalyst prepared by precipitation (80 °C to evaporate water, and heated at 1000 °C in air for 6 h) to form ferric oxide catalyst precursor	Acetylene (0.05 sccm) and H_2 (0–0.03 sccm)	450 °C at atmospheric pressure, reaction time of 6 h	CVD. Horizontal quartz tube (60 mm inner diameter and length 800 mm), equipped with temperature and gas controllers
Qi et al. [60]	Helical carbon nanotubes with single, double and triple intertwined carbon nanotubes, tube diameter 100–150 nm and coil diameters and coil pitches of 0.5–4.0 μm and 0–2.0 μm (single), 500 nm and 0–50 nm (double). Wormlike carbon nanocoils and coiled carbon nanobelts	Ferric oxide catalyst particles prepared by precipitation (heated at 1000 °C in air for 6 h). Grain sizes determined after synthesis of carbon structures (40–100 nm)	Acetylene, H_2 (none during synthesis)	450 °C at atmospheric pressure, reaction time 4 h	CVD. Horizontal quartz tube (60 mm inner diameter, length 800 mm), equipped with temperature and gas controls
Tang et al. [37]	Helical carbon nanotubes and fibers with diameters of 100–200 nm. Twin helical nanotubes/fibers that grow symmetrically from a single catalyst particle	Fe xerogel catalyst prepared from ethanol at 60 °C for 6 h, and calcined at 450 °C for 3 h. Particle size altered by amount of raw material used	Acetylene and H_2	475 °C at atmospheric pressure, reaction time 1 h	CVD. Quartz reaction tube (50 × 350 mm tube), placed inside steel reactor (52 × 800 mm) equipped with temperature and gas-flow controls
Daraio et al. [61]	Foam like forest of aligned coil-shaped carbon nanotubes. Coil diameter of 20 nm and coil pitch of 500 nm, with parallel graphene walls creating a tube	Indium isopropoxide dissolved in xylene ferrocene mixture. Atomic concentration of Fe was − 0.75 and 1%, while indium concentration varied systematically	Acetylene (50 sccm), Ar (800 sccm), xylene/ferrocene/ indium isopropoxide (injected at 1 mL/h)	700 °C at atmospheric pressure.	CVD. Two stage reactor, comprising of liquid and gas injectors
Kong et al. [62]	Straight (80%) and helical (5%) carbon nanotubes (diameters 20–60 nm). Some helical nanotubes had variable pitches and some composed of bamboo structures	Ferrocene	Polyetylene glycol (carbon source)	700 °C, reaction time of 12 h	Autoclave (stainless steel, 20 ml), sealed and placed in electronic furnace
Hokushin et al. [36]	Carbon nanocoil tubules, ranging between 50–100 nm	$M(COOH)_n$ (M = Fe, Sn, In), dissolved in ethanol and toluene and spin coated on Si substrates and sintered at 450 °C in air	Acetylene (30 sccm) and He (260 sccm)	700 °C	CVD
Wang et al. [63]	Helical carbon nanotubes, double helix (tube diameters 15–25 nm, with pitch of 1 μm) when In used. Helical carbon nanowires when Sn used	Fe-In and Fe-Sn catalysts, prepared by indium isopropoxide dissolved in xylene-ferrocene mixture (C:Fe:Sn, 99:0.25:0.75) and tin isopropoxide dissolved in xylene-ferrocene mixture (C:Fe:In, 99:0.80:0.20)	Acetylene (50 sccm), Ar (80 sccm), xylene-ferrocene mixture (containing In and Sn sources) injected	200 °C (first stage), 700 °C second stage, reaction time of 1 h	CVD. Two stage thermal reactor, equipped with syringe pump

(*continued on next page*)

Table 1 (*continued*)

Reference	Tubes/tubules				
	Type of carbon	Catalyst	Gas atmosphere	Temperature (°C)	Reactor
Li et al. [50]	Carbon nanocoils with more than two tubules twisted around each other, with coil diameters of 500–700 nm and coil pitches of 300–600 nm. Structure of tubules is amorphous	Fe–Sn–O catalyst prepared by sol gel, from ethanol at 80 °C for 3 h and calcined at 700 °C for 3 h. Dispersed on Si substrate for carbon fiber synthesis. Fe:Sn ratio was estimated to be 15:6 from EDX analysis	Acetylene diluted with Ar with total flow rate of 260 sccm	700 °C at atmospheric pressure, reaction time 30 min	CVD. Horizontal quartz tube
Hernadi et al. [64]	Coiled carbon nanotubes, spirals are definite nanotubes, well graphitized with hollow core. Tube diameters vary (depending on pH) 10–100 nm, with coil pitches of 10–300 nm	Co supported on silicagel, prepared by precipitation at varying pH values	Acetylene (10 sccm) and N_2 (70 sccm)	720 °C, at atmospheric pressure, reaction time of 30 min	CVD
Fejes et al. [65]	Spiral carbon nanotubes. Spirals favoured using impregnation method and zeolite, as opposed to $CaCO_3$; additionally treatment of ball milled samples with ammonia increased the yield of spirals	Co supported catalysts, prepared by crystallization from supersaturated solutions, impregnation using $CaCO_3$, 13X zeolite, silicagel, as well as by ball milling (using Fe and Co precursors and supports)	Acetylene (10 sccm) and N_2 (500 sccm)	720 °C, at atmospheric pressure, reaction time of 30 min	CVD. Fixed bed flow reactor
Cheng et al. [66]	Coiled carbon nanotubes (regular), with a variety of radii and coil pitches. Carbon nanotubes intertwine to form tight triple helices (or braids)	Manganese oxide (mineral) containing Fe and minute amount of Ni	Acetylene (100 sccm) and N_2 (500 sccm)	750 °C, at atmospheric pressure, reaction time of 15 min	CVD. Horizontal quartz reactor
Zhang et al. [67]	Carbon nanotube-array double helices (self-organization of carbon nanotubes into an ordered 3D double helix structure). Some cases helical carbon nanofibers were also observed	Fe/Mg/Al layered double hydroxide catalyst flakes, prepared by co-precipitation	Acetylene (300 sccm), Ar (100 sccm) and H_2 (50 sccm)	750 °C, at atmospheric pressure, reaction of 30 min	CVD. Horizontal quartz tube (25 mm inner diameter), heated by electric furnace
Somanathan et al. [68]	Helical carbon nanotubes (multi-walled), composed of two to three-coiled nanotubes (tube diameters of 20–30 nm), which are well graphitized	FeMo/MgO catalyst, prepared by combustion method using metal precursors, solution containing precursors was fed into a furnace at 550 °C for 5 min. Reduction at 800 °C under H_2	Acetylene (60 sccm), N_2 (200 sccm) and H_2	800 °C	CVD. Horizontal quartz reactor
Zhong et al. [69]	Coiled carbon nanotubes, pitches and coil diameters range between 100 and 300 nm	Iron oxide film deposited on Si substrate (patterned to 40 μm using photolithography). Aligned CNTs grown and dipped in $Fe(NO_3)_3$ solution and heated to 400 °C in air	Methane and N_2, flow rate ratio 1:4	–	Microwave plasma enhanced CVD

Table 2 Synthetic parameters related to the synthesis of helical carbon fibers.

Reference	Fibers				
	Type of carbon	Catalyst	Gas atmosphere	Temperature (°C)	Reactor
Sevilla et al. [70]	Carbon nanocoils, long curled ribbon of carbon with diameters of 70–100 nm. Highly graphitic, crystalline	Ni catalyst prepared by impregnation of Ni salt onto hydrochar samples using ethanol	Saccharides (glucose, sucrose, starch) hydrothermally carbonized to obtain hydrochar that was then graphitized to produce carbon coils	180–240 °C (to produce hydrochar). 900 °C, reaction time 3 h	Saccharides carbonized in Teflon-lined autoclave. Impregnated hydrochar heat treated at 900 °C in N_2
Ren et al. [71]	Helical carbon nanofibers (regular). Bimodal symmetric growth (diameter 80–100 nm). Cu/MgO produces highest yield of helical carbon nanofibers	Cu supported catalyst prepared by conventional impregnation (MgO, SiO_2, Al_2O_3, TiO_2), dried at 80 °C and calcined 600 °C for 5 h. Reduced at 550 °C in H_2	Acetylene	194–250 °C, at atmospheric pressure	CVD. Horizontal quartz tube (60 × 900 mm), heated by electric furnace
Yu et al. [72]	Helical carbon nanofibers (regular). Bimodal symmetric growth (diameter 100 nm)	Cu-Ni catalyst, prepared by hydrogen arc plasma	Acetylene	241 °C, at atmospheric pressure	CVD. Horizontal quartz tube (90 × 900 mm), heated by electric furnace
Qin et al. [14]	Helical carbon nanofibers (regular). Bimodal symmetric growth (diameter 50 nm). Metal salt precursor did not have an effect on morphology of carbon fibers. Ribbon-like fibers by arc plasma	Cu catalyst, prepared by precipitation of copper tartrate/butyrate/oxalate/lactate, as well as borohydride reduction and hydrogen arc plasma	Acetylene	250 °C, under vacuum, reaction time of 30 min	CVD. Horizontal quartz tube (90 × 900 mm), heated by electric furnace
Shaikjee et al. [73]	Helical carbon nanofibers (regular). Bimodal symmetric growth (diameter 50–200 nm). Catalyst and pre-treatment conditions (reduction temperature) affect type of fiber obtained	Cu/TiO_2, Cu/MgO, Cu/CaO, prepared by deposition-precipitation of Cu salts dissolved in various solvents. Catalysts reduced at various temperatures inferred from TPR data	Acetylene 100 sccm and H_2 100 sccm	250 °C	Approximately 500 mg of catalyst material was uniformly spread onto a small quartz boat, and placed in the centre of a horizontal furnace, that was heated by an electric element
Jian et al. [74]	Twin helical nanofibers (mean fiber diameter of 50 nm) that grow symmetrically from a single catalyst particle. Straight carbon fibers obtained at heating rates above 3 °C/min under argon	Catalyst precursor, copper (II) tartrate prepared by precipitation. Particles shapes are irregular with mean grain size of 50 nm	For helical fiber-acetylene; for straight fibers-addition of argon	271 °C at atmospheric pressure, 15 min reaction time, variable heating rates	CVD. Ceramic boat with catalyst placed in quartz tube (45 × 1300 mm) at atmospheric pressure
Fukuda et al. [75]	Carbon coils, with fiber diameters of 50–300 nm and coil diameters of 100–3000 nm	An alloy rod composed of Fe:Cr:Ni (74:18:8)	Benzene at critical temperature and pressure	290 °C	Benzene placed in a stainless steel container and irradiated with an ultraviolet laser (3.9 mW mm^{-2}) CVD.

(*continued on next page*)

Table 2 (*continued*)

Reference	Fibers				
	Type of carbon	Catalyst	Gas atmosphere	Temperature (°C)	Reactor
Zhou et al. [40]	Carbon micro-cols (super hydrophobic). At first carbon microcoils grow from thin filaments (10 nm), at 12 min coils appear curled together, at 24 min coils grow longer with diameters of 100–400 nm. The pitch became larger with time	Cu catalyst, prepared by electro-oxidation of copper to form copper tartrate precursor, precursor was later heated to 400 °C in vacuum to yield catalyst	Acetylene and N_2	400 °C, at atmospheric pressure, reaction time of 24 min	CVD
Kawaguchi et al. [42]	Double helix regular carbon micro-coils	Ni powder (mean diameter 5 μm)	High purity acetylene and commercially dissolved acetylene, as well as addition of small amounts of acetone, oxygen, water, carbon monoxide, ammonia and thiophene	300–1000 °C, at atmospheric pressure	CVD. Horizontal quartz tube (40 × 1000 mm)
Chesnokov et al. [76]	Twisted filamentous carbon, with bimodal symmetrical growth from single catalyst particle	Ni-Cu/MgO catalyst (carbonized)	1,3-Butadiene (carbon source), Ar and H_2 (ratio of 2:40:75 respectively)	450 °C, at atmospheric pressure	CVD
Tang et al. [77]	Carbon nanocoils (coil diameters 120–500 nm), regular and tight with short pitch. Coils appear as spring-like or plait-like bundles	Ni xerogel catalyst prepared from ethanol (60 °C for 4 h), heated at 400 °C in air for 4 h, to yield NiO_x catalyst precursor	Acetylene and H_2	450 °C, at atmospheric pressure, time of reaction 1 h	CVD. Horizontal quartz tube (53 × 850 mm), equipped with temperature and gas controllers
Liu et al. [34]	Carbon nanocoils (twisted), with coil diameters of 100–300 nm and coil pitches variable. Carbon nanocoil (wire), coil diameter 200 nm and coil pitch 100 nm	Ag nanoparticles were prepared by sputtering on Si substrate. K vapour was obtained by thermal decomposition of KH to form a K layer on silicon substrate	Acetylene (3 sccm), H_2 (20 sccm) and Ar (20 sccm)	450 °C at atmospheric pressure, reaction time 15 min	CVD. Reactor composed of Lindberg HTF55122A tube furnace with 28 mm diameter quartz tube

Jia et al. [78]	Twisted carbon nanofibers (500 °C), Helix branched shaped fibers (low yield, 700 °C) with diameters of 50–100 nm	K catalyst prepared by grinding KI into paste followed by addition of polystyrene solution under grinding, the catalyst precursor was then dried at 60 °C for 10 h	Acetylene (50 sccm) and N_2 (50 sccm)	500–700 °C, under vacuum, reaction time 1 h	CVD. Quartz reaction tube
Qin et al. [79]	Helical (and straight) carbon nanofibers with diameters 100–200 nm (Li). Helical (and straight) carbon nanofibers (Na). High yield helical carbons (and some twisted forms) with diameter 100 nm (K). Some helical carbons with Cs	Alkali catalysts, prepared from alkali chloride catalysts (LiCl, NaCl, KCl and CsCl). Alkali chlorides ground with toluene solution containing polystyrene, dried at 60 °C for 8 h. Calcined at 600 °C in air fro 1 h	Acetylene (50 sccm)	500–700 °C, under vacuum, reaction time 1 h	CVD
Ivanov et al. [80]	Coiled carbon nanotubules (diameter 10 nm), obtained from Co/SiO_2 catalyst	Fe, Co, Ni, Cu supported catalysts, prepared by impregnation on graphitic flakes and ion exchange on silica. Catalysts were dried overnight and calcined at 500 °C for 2 h	Acetylene (2.5–10%) and N2	500–800 °C, at atmospheric pressure, reaction times of several hours	CVD. Flow reactor with quartz tube (4×600 mm)
Motojima et al. [81]	Double and triple stranded carbon micro-coils. Cross section of the coils reveal that they were mostly circular or elliptical. Optimum coil yield obtained with addition of 0.01 sccm PH_3 and reaction temperature of 600–700 °C	Ni powder with mean diameter of 5 μm. Dispersed on graphite plate during reaction. Ni–P prepared by addition of small amounts of PH_3 during reaction	Commercial acetone-dissolved acetylene (30 sccm), H_2 (70 sccm) and Ar (40 sccm)	550–800 °C at atmospheric pressure	CVD. Horizontal quartz tube (40 mm inner diameter), with reaction tube heated by nichrome elements
Wang et al. [82]	Helical carbon nanofibers (regular). Bimodal symmetric growth with fiber diameter 50–80 nm, coil diameter of 80–100 nm and coil pitch of 80–120 nm	Ni substrate treated with $SnCl_2$ precursor	Ethanol	580–640 °C, flame (20×50 mm), reaction time of 5–10 min	Flame synthesis. Laboratory ethanol burner, with substrate facing down above the flame (20 mm above)
Lu et al. [83]	Twisted and helical carbon fibers at low H_2 concentrations. Tight helical fibers at CO concentration of 58.3%. Twisted carbon nanofibers at 645 °C	Fe_2O_3 catalyst (particle size 20–30 nm)	CO (carbon source), H_2 and Ar (total flow rate 120 sccm)	600–645 °C, at atmospheric pressure	CVD
Yang et al. [84]	Four types of carbon coils: unsupported (650–800 °C) Irregular carbon micro-coils, unsupported (700–750 °C) single helix carbon micro coils, supported (750–790 °C) super elastic carbon micro-coils, supported (650–750 °C) single helix carbon microcoils	Ni-Fe-Cr alloy catalysts with/without ceramic support. Metal salts mixed with molecular sieve powder (60 °C for 2 h), dried (100 °C for 12 h) and calcined (500 °C for 3 h). Reduced and activated in H_2 for 1 h at 700 °C. Dispersed on graphite substrate during reaction	Acetylene (30–150 sccm), H_2S/H_2 (10–200 sccm), H_2 (50–550 sccm) and N_2 (0–100 sccm)	600–800 °C at atmospheric pressure	CVD. Vertical quartz tube (60 mm inner diameter), with upper gas inlet and lower gas outlet, with reaction tube heated by nichrome elements

(*continued on next page*)

Table 2 (*continued*)

Reference	Fibers				
	Type of carbon	Catalyst	Gas atmosphere	Temperature (°C)	Reactor
Yang et al. [85]	Regular single helix carbon micro-coils. Carbon fiber diameter of 0.5–1 μm, coil diameter of 1–3 μm and coil pitch of 1–3 μm	Fe-Ni alloy supported catalyst. Impregnated deposits were dried (100 °C for 12 h) and calcined (500 °C for 3 h). Ratio of Fe versus Ni was varied. Dispersed on graphite substrate during reaction	Acetylene (60 sccm), H_2S/H_2 (20–50 sccm), H_2 (200 sccm) and N_2 (75 sccm)	600–850 °C, with optimum at 800–820 °C at atmospheric pressure, reaction time 30 min	CVD. Vertical quartz tube (60 mm inner diameter), with upper gas inlet and lower gas outlet, with reaction tube heated by nichrome elements
Pan et al. [46]	Carbon nanocoils, single and double helix, with various diameters and pitches, with fiber diameters ranging from several tens to several hundreds of nm	Substrate indium tin oxide film (300 nm), patterned with Fe films thickness (15 and 100 nm) formed by vacuum vaporization using shadow masks	Acetylene (30–60 sccm) and He (200 sccm)	620–750 °C, at atmospheric pressure, reaction time of 5–60 min	CVD. Horizontal tubular electric furnace
Hanus et al. [86]	Twisted carbon fibers, fiber diameters of 200–500 nm. The twisted carbon fibers consist of four helical strands (two small diameter strands interspaced with 2 large diameter strands, tightly wound)	$NiSO_4/Al_2O_3$ (1:20) prepared by wet impregnation, dried at 60 °C for 18 h and calcined in air at 500 °C for 5 h	Acetylene and H_2 (3:1, total flow rate of 6 sccm). H_2 and N_2 (1:4, total flow rate of 6 sccm)	650 °C	Fluidized-bed reactor. Vertically aligned reactor tube (0.052 × 1 m, incolnel 601), located within an electrically-heated furnace with stainless steel distributor plate located at the bottom of the tube
Bi et al. [87]	Carbon microcoils (3D helical structure with coil diameters and pitches of 5.5–9.0 μm and 1.0–1.5 μm) and wave-like carbon fibers (diameters 100–200 nm. Both forms have moderate degree of graphitization	Ni–P catalyst, prepared by four-stage electroplating of the surface of a graphite substrate. Appears as cauliflower-like grains with mean particle size of 1–5 μm. EDX analysis reveals P content of 8.5%	Gas mixture of commercial acetylene (dissolved in acetone), with small addition of thiophene (promoter), hydrogen and nitrogen, with flow rates of 30, 40, 90 sccm respectively	650–800 °C at atmospheric pressure. Reaction time 1.5 h	CVD. Horizontal quartz tube (25 × 1200 mm) in electric furnace
Yang et al. [88]	Twisted carbon nanocoils with coil diameters of 100–400 nm (TiC). Carbon micro (several μm coil diameters) and nanocoils (100–400 nm coil diameters) using TiN. Twisted carbon nanocoils with coil diameters of 100–600 nm ($NiTiO_3$)	Various Ti catalysts with grain diameters of 0.5–1.5 μm	Acetylene (60 sccm), H_2 (100 sccm), N_2 (100 sccm) and H_2S/H_2 (90 sccm)	660 °C, at atmospheric pressure	CVD. Horizontal quartz tube (30 × 700 mm), equipped with temperature and gas controllers
Yang et al. [89]	Tile-like (diameters of 0.5–2 μm) and zigzag (diameters of 200–400 nm) carbon nano/micro-fibers. Are in fact 2-D helical fibers	Fe/Al_2O_3 catalyst, prepared by deposition precipitation. Reduced under vacuum at 600 °C for 3 h	Acetylene (160–330 sccm), H_2 (200–400 sccm) and H_2S (diluted in H_2, 5–50 sccm)	700–800 °C, at atmospheric pressure, reaction time 20 min	CVD. Vertical reaction system with upper gas inlet and lower gas outlet
Chang et al. [90]	Carbon nanocoils with fiber diameter of 100–300 nm, coil diamater of 300–1200 nm and coil pitch of 600–1800 nm. Coils have tubular structure but not as cylindrical as CNTs	Stainless steel plates (Cr 18%, Ni 8%) with fine polished surfaces, upon which $Sn(C_2H_2O_2)_2$ is spun, and then oxidised at 500–900 °C in air for 30 min	Acetylene (5 sccm) and Ar (600 sccm)	700 °C, at atmospheric pressure, time of reaction 30 min	CVD. Horizontal quartz tube (25 mm inner diameter)

Bi et al. [91]	Regular single fiber carbon nanocoil (76% selectivity). Tightly twisted coil morphology, without central void. Coil diameters of 450–550 nm and fiber diameters of 100–400 nm. Other forms of carbon include straight fibers, helical carbon microcoils and shapeless amorphous deposits	Co–P catalyst, prepared by electroless plating on graphite substrate. Appears as cauliflower-like grains with mean particle size of 350 nm. EDX reveals P content of 6.9%	Gas mixture of acetylene, with small addition of thiophene, hydrogen and nitrogen, with flow rates of 20, 40, 80 sccm respectively	700–900 °C at atmospheric pressure. Reaction time 20 min	CVD
Liu et al. [92]	Coiled carbon nanofibers, regular double helix with diameters of 50 nm (individual fibers 21 nm). Also braids (regular), which appear as if partially rolled up from a single layer (diameters 10–several hundred nm)	Fe nanoparticles embedded in mesoporous silica. Prepared by sol-gel (iron nitrate and TEOS), dried at 60 °C for 1 week and calcined at 450 °C under 0.1 Torr for 10 h. Reduced at 550 °C for 5 h	Acetone (carbon source) and H_2, (bubbled through acetone at 500 sccm)	715 °C, at atmospheric pressure, reaction time 30 min	CVD
Chen et al. [43]	Double helix carbon micro-coils, circular and flat cross sections, with some conically coiled flat carbon coils	Ni powder (5 μm mean diameter), dispersed on a substrate	Acetone dissolved commercial acetylene, H_2, N_2 and thiophene as growth promoter	750 °C, at atmospheric pressure, reaction time of 1–2 h	CVD. Horizontal quartz tube (30 mm inner diameter), heated by AC electric heater
Banerjee et al. [93]	Coiled carbon fiber in thin film form, with diameters ranging from 0.1–1 μm, with large coiled fibers having coil pitches of 500 nm	Ni catalyst, prepared by dip coating of purified Cu substrate into Ni solution	Acetylene	750 °C (substrate temperature), deposition pressure maintained at 10 mbar, reaction time 15 min	Plasma enhanced CVD. Deposition carried out at a dc voltage of 2 kV and the corresponding current density ~25 mA/cm^2
In-Hwang et al. [53]	Regular coiled carbon coils (coil diameter 4–6 μm) without substrate rotation. Slightly irregular carbon coils with rotation	Ni catalyst dispersed on graphite plate	Acetylene, H_2, N_2 and thiophene	770 °C, at atmospheric pressure, time of reaction 2 h	CVD. Horizontal and vertical quartz reaction tubes (55 mm inner diameter) with rotating holder (0–180 rpm)
AuBuchon et al. [54]	CNTs with zigzag morphology, each bend 90 °, with segments 500 nm in length	Ni sputter deposited on Si substrate	Acetylene (30 sccm) and NH_3, total gas pressure of 3 Torr	780 °C	DC plasma enhanced CVD. DC bias voltage of 550 V below the sample and DC self-bias potential at 10 V with electric field magnitude of 0.1 V/μm
Yong et al. [45]	Heterostructured helical carbon nanotubes, diameters of 100–200 nm	Quartz plate dipped in $Fe(NO_3)_3$ solution and dried at room temperature	Ethanol (injection)	800 °C	CVD. Horizontal quartz tubulat furnace
Zhang et al. [32]	At 160 Torr mostly straight fibers with fraction of micro-coils (coil diameter of 0.5–0.8 μm and coil pitch of 0.8–1.2 μm. At 385 Torr majority of carbon deposit is double helical material with coil diameter 6–10 μm. At 460 Torr mainly straight fibers with diameters of 50–100 nm	Ni plate provided catalyst particles	Industrial grade acetylene	–	Arc discharge. Pure graphite rod (12 × 200 mm) and metal plate (80 × 80 × 15 mm) used as anode and cathode. The arc was generated with output current of 96 A and voltage of 35–40 V in acetylene atmosphere at 160–460 Torr

be expanded by 200%, with measured elastic spring constants ranging from 0.01 to 0.6 N/m and a Young's modulus of ~ 0.1 TPa (approx. 0.1 times that of CNTs).

Chen et al. [96] further investigated the mechanical response of carbon coils under direct tensile loading. The ends of a single carbon coil were attached to two AFM tips; one was kept static and the other compliant, Fig. 18. It was found that the carbon coil could be extended to a maximum relative elongation of 33% without any plastic deformation after the tensile load was released. The nano-coil spring constant, defined as the total applied load (determined from a cantilever spring constant) divided by the total elongation was found to be 0.12 N/m. The shear modulus, determined by fitting to equations that express the spring constant in terms of the coil geometry and shear modulus, was calculated. It was found that the theoretical analysis was consistent with the experimental data, Fig. 19. Furthermore Chen et al. [96] were able to show that the shear modulus for coiled nano-tubules (2.5 GPa) is much lower than that of CNTs (estimated at 400 GPa).

More recently Bi et al. [98] considered the elastic properties of carbon coils with circular cross-section grown over a Ni–P alloy catalyst at 700 and 750 °C using C_2H_2 as the carbon source and thiophene as an additive. It was observed that these CMCs could be easily extended to an almost linear shape without any noticeable damage to their fiber structure, even after one week of extension under atmospheric conditions, Fig. 20. It was also observed that as the coil was stretched the pitch increased while the coil diameter decreased (became linear). Based upon their experimental observations, Bi et al. [98] were able to develop a set of equations that could predict spring constants and load elongation responses for carbon materials with spring-like structure, thereby producing a model that could be used for the development of micro/nano-devices.

Poggi et al. [99] were able to demonstrate that MWCNT coils, did not just exhibit extension behaviour but compression behaviour as well. They showed that a 1100 nm length of coil could undergo compression/buckling/decompression repeatedly with a limiting compression of 400 nm. However when compared to modelled data the nanotube spring stiffness was found to be 6x lower than that predicted (0.7 N/M measured, 4 N/M predicted), which they attributed to experimental interferences. Chang and Chang [100] were able to confirm the

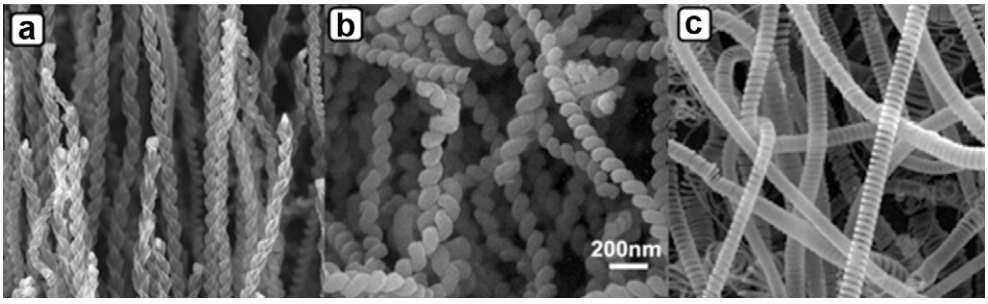

Fig. 17 Types of helical carbon nanomaterials produced: (a) twisted helices [50] (b) tightly coiled helices [35], (c) spring-like coils [87].

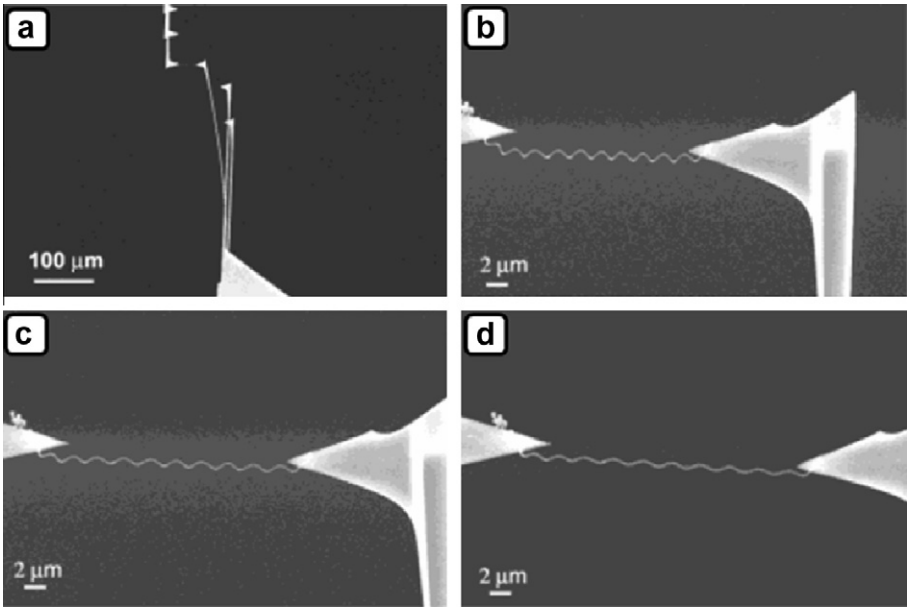

Fig. 18 Carbon nanocoil clamped between two AFM cantilevers: (a–d) Elongation of nanocoil upon tensile loading (relative elongation of 33%) [96].

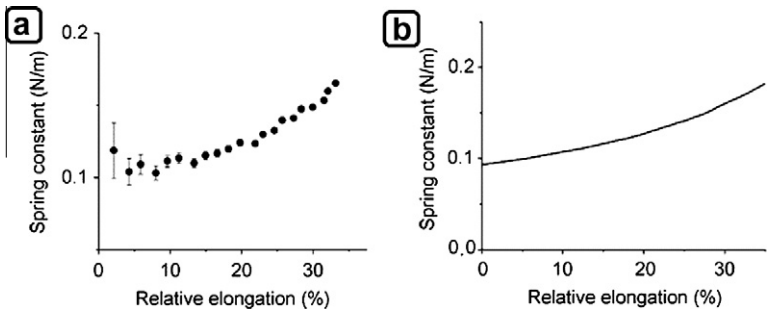

Fig. 19 Plots of relative elongation vs. spring constant: (a) experimental observations, (b) theoretical analysis [96].

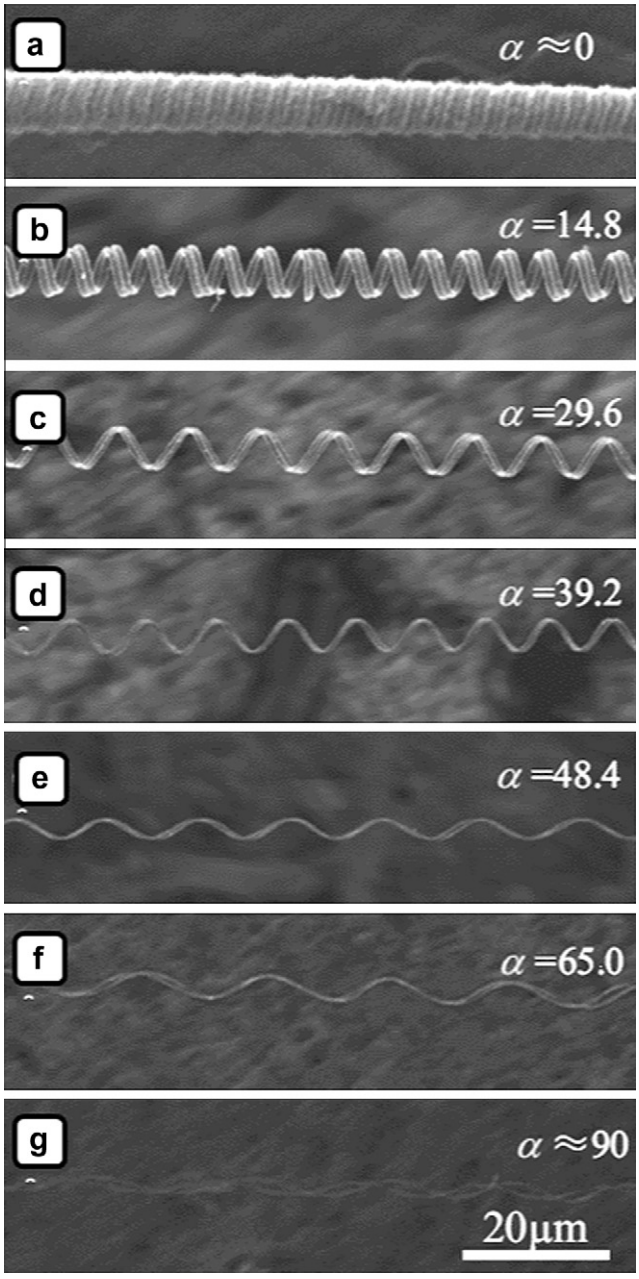

Fig. 20 Elongation of carbon coils: (a–g) coil pitch increases while coil diameter decreases until almost linear [98].

compression and extension behaviour of carbon coils, by exposing CMCs to lateral force microscopy studies. By placing the AFM tip a certain distance along the CMC, they were able to show that the spring constant for CMCs was dependent upon the number of active coils. While researchers considered the mechanical response of individual coils or springs (nano and micro), Daraio et al. [61] examined the response characteristics of a foam-like forest of coiled carbon nanotubes. By using a drop ball test, Fig. 21a, they were able to show that the coiled forest revealed no plastic deformation when struck, and retained its original state when the force was removed (elastic deformation). The total depth displacement into the coiled forest was estimated at ~3 μm, with an interaction area of ~77 μm and a pressure estimated at ~16 MPa. The coiled CNTs appeared to act as a cushion protecting the bottom wall (sensor). The coiled CNTs reduced the pulse amplitude and increased its length as compared to a bare quartz substrate, Fig. 21b.

Furthermore they observed that the elastic behaviour persisted even after repeated high velocity impacts, despite the appearance of cracks on the film surface. They compared the elastic deformation characteristics of coiled carbon nanotubes with that of straight carbon nanotubes (similar foam-like forest) and observed that the straight CNTs showed permanent plastic deformation and densification around the impacted area. They concluded that the elastic behaviour of coiled CNTs was significantly superior to that of straight CNTs and could be an effective component in nano scale systems.

The resonance capabilities of coiled CNTs were investigated by Volodin et al. [101] using coiled CNTs as self-sensing mechanical resonators. Coiled CNTs were attached to gold electrodes, and this device was then connected to a compact radio frequency circuit (frequency range between 50 and 400 MHz), as well as an ultrasonic transducer (for acoustic excitation). They observed that the resonance frequency of these tiny mechanical devices were in the microwave GHz regime. Furthermore, these sensors were found to be suitable for measuring small forces and masses in the femtogram range.

Electrical behaviour

The unique properties associated with coiled carbon materials were further investigated by Kaneto et al. [102] who showed as far back as 1999 that carbon micro-coils displayed intriguing electrical behaviour. By conducting a set of elegant experiments they were able to show that CMCs possessed electrical

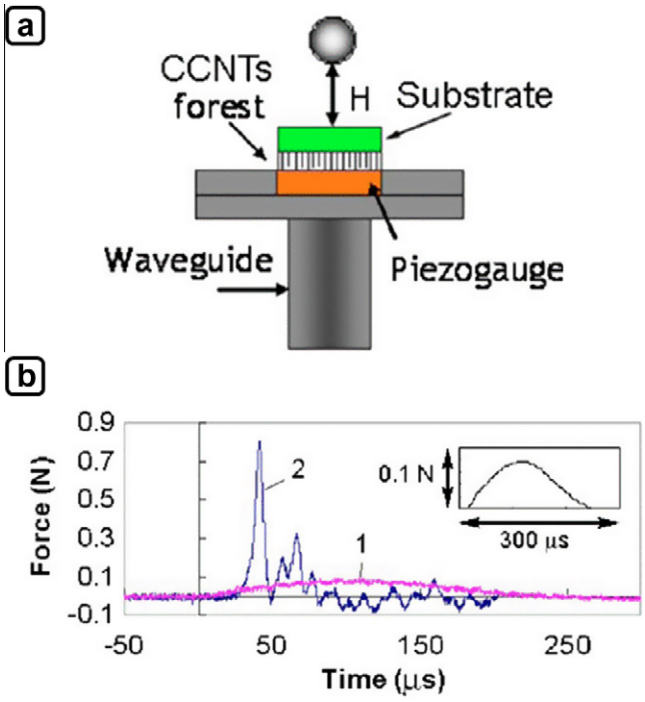

Fig. 21 (a) Schematic representation of device setup, with coiled CNTs acting as shock absorber (between substrate and sensor), (b) impact response with coiled CNTs (curve 1 – purple) and without coiled CNTs (curve 2 – blue) [61].

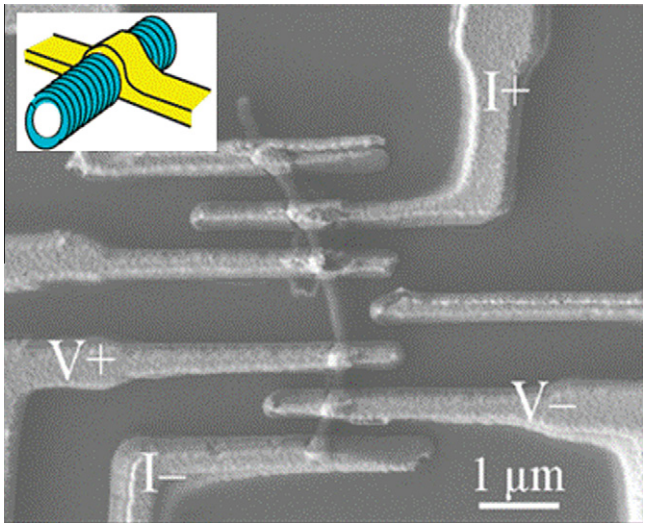

Fig. 22 Electrical nano-device with carbon coil providing electrical contact [77].

conductivities of 30–50 S/cm, and that the conductivity increased by 5–20% upon evacuation of the atmosphere. A 1–2% increase in conductivity was noted upon exposure to iodine gas (oxidative atmosphere) but the value was unchanged when exposed to ammonia gas (reductive atmosphere). They were also able to conclude that the conductivity temperature dependence indicates both conductive and semi-conductive behaviour, and shows a mechanism for electron transport

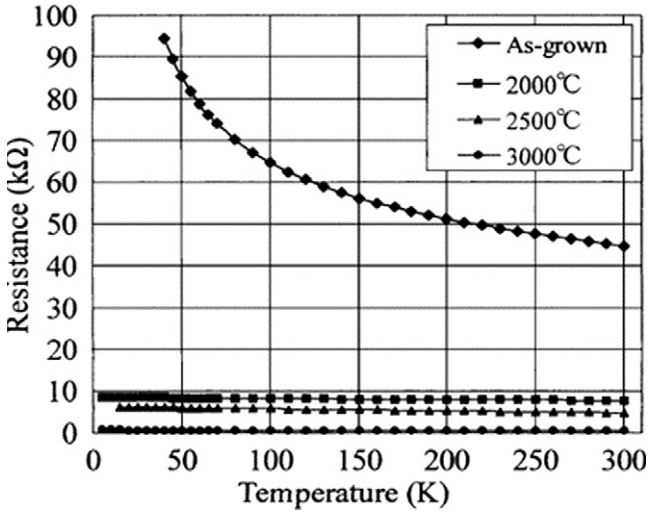

Fig. 23 Temperature dependence of the resistance for carbon coils annealed at various temperatures [105].

Table 3 Comparison of field emission characteristics of different carbon structures as reported by Banerjee et al. [93].

Type of carbon field emitter	Turn on field (V/μm)
Horizontal aligned CNT	2.2
CNT films treated using H_2 plasma	1.2–0.5
Horizontal aligned CNT	2.0–1.8
CNT pillar arrays	2.9–0.9
Aligned CNF	5.1–2.6
Branched CNT film	8.1–6
Carbon nanoneedle	17.1–3.8
Triode-type CNT emitter arrays	20–16.4
Vertically aligned carbon nano-rope	15
Fe-core CNT	9–5
Carbon coil	4.5–1.96

(conductivity) that was indicative of a 3D variable range hopping model. The 3D electron hopping model was supported by Chiu et al. [103] who showed that the temperature dependant resistance analyzed by the Efross–Shklovskiu VRH conduction model, was indicative of 3D electron hopping conduction, with an electron hopping length of $\sim$ 5 nm. Studies by Tang et al. [77] confirmed this proposal and demonstrated a possible electron hopping length of 5–50 nm. Their studies also showed an effective route to improve electrical contacts in nanodevices, Fig. 22, by focused laser annealing, providing for an ideal route to single-nano-wire devices. Liu et al. [104] considered the electrical conductivity of mats made of coiled carbon fibers impregnated with Pd metal clusters, and found that they showed variable-range hopping characteristics and thermo-power behaviour reminiscent of some conducting polymers. Hayashida et al. [97] were able to show, by bridging a single coiled carbon nano-tubule between two tungsten needles, that the degree of graphitization affected the conductivity. It was observed that the coiled carbon nano-tubule exhibited electrical conductivities of $\sim$ 180 S/cm (less than the conductivity of a CNT), whereas the amorphous carbon micro-coil was found to have conductivities of $\sim$100 S/cm.

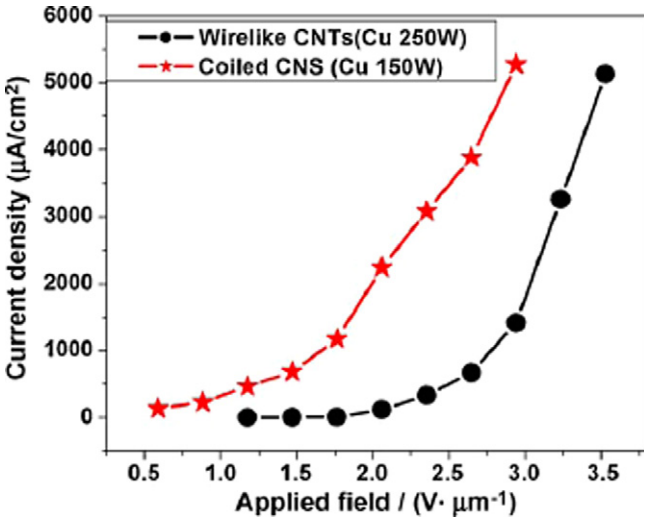

Fig. 24 Field emission properties of coiled carbon nanomaterials and straight (wirelike) CNTs [108].

Fujii et al. [105] were able to demonstrate that as the annealing temperature of the carbon micro-coils was increased (from 2000 °C to 2500 °C and 3000 °C) resistivity decreased, Fig. 23. They postulated that this was due to the increased number of mobile carriers due to the increased graphitization of the materials at higher temperature. However the annealing temperature not only affected the resistivity but also the magnetoresistance, which decreased with increasing annealing temperature. Furthermore they were able to show that the difference in magnetoresistance under a parallel and/or transverse magnetic wave was due to the morphology of the carbon material, and that this meant current flowed helically along the carbon fiber (micro-coil). Kato et al. [106] observed that when CMCs were exposed to alternating currents of different frequencies, the CMCs expanded and contracted as the current flowed through. They also observed that for a clockwise coil, the CMC expanded when the negative amplitude reached a maximum and contracted when the positive amplitude reached a maximum (the reverse was seen for an anti-clockwise coil). This phenomenon was attributed to the electromagnetic properties of the CMC owing to its spiral morphology.

Field emission behaviour

In order to determine the field emission properties of thin film carbon micro/nano-coils, Banerjee et al. [93] carried out field emission measurements using a diode configuration consisting of a cathode (the thin film) and a stainless steel anode. By varying the inter electrode distance, they were able to show that coiled carbon structures showed moderately good field emission properties with a turn on field of 1.96 V/μm (defined in terms of current density increasing by a significant value of 2 $\mu A/cm^2$) for an inner electrode distance of 220 μm. They also showed that, when compared to other studies, Table 3, carbon coils have a comparable turn-on field similar to that of other carbon based nanostructures. Zhang et al. [107] considered the field emission properties of carbon nano-helices, and found that a field emission current density of 1 mA/cm^2 is achieved at

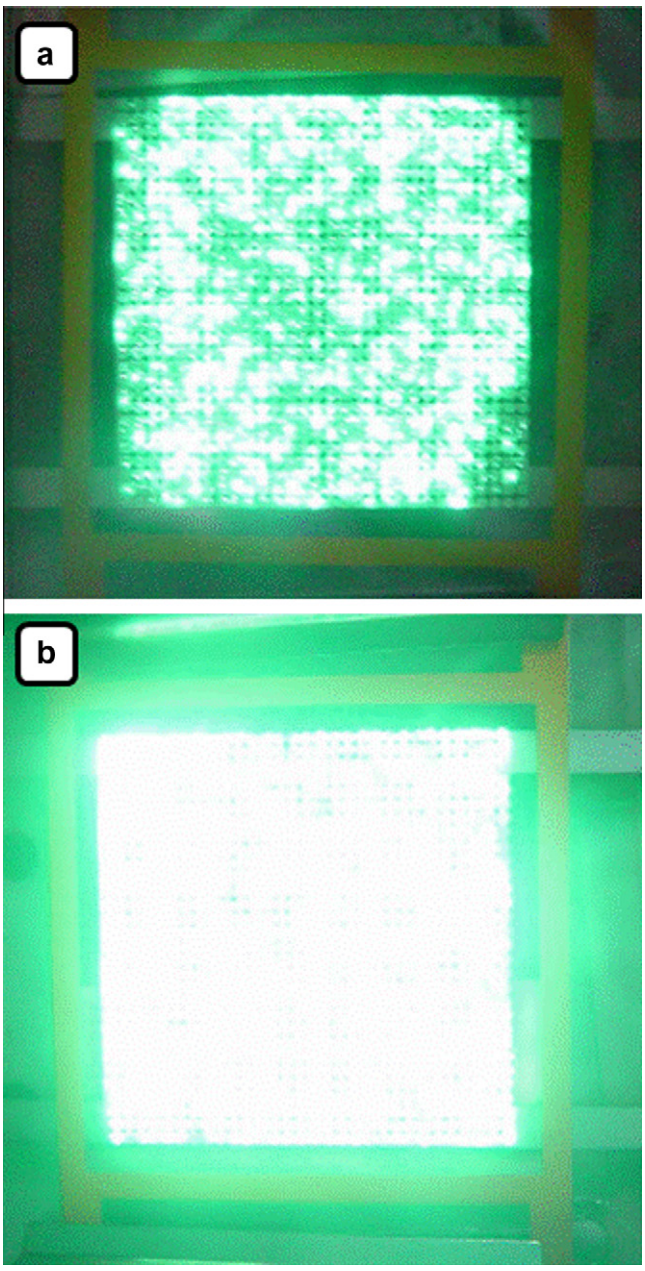

Fig. 25 Electron emission images of: (a) straight CNTs, (b) coiled carbon nanomaterials at the same applied electric field [108].

~1700 V and a current density of 10 mA/cm^2 at ~2100 V. They concluded that the carbon nano-helices show excellent field emission properties (which can be attributed to the large number of emission sites formed by the tips and edges of the carbon nano-helices) and are comparable to those of carbon nanotubes.

Zhang et al. [108] were able to show that compared to straight CNTs, coiled carbon nanostructures showed higher field emission properties. Fig. 24 shows that at the same applied voltage straight CNTs have a lower current density as compared to the coiled carbon nanostructures. Furthermore at the same applied electric field the coiled carbon nanostructures have

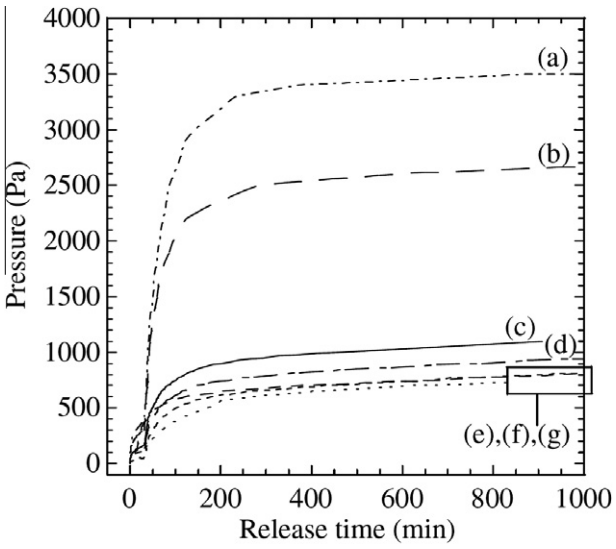

Fig. 26 Hydrogen desorption behavior of various carbonaceous materials: (a and b) two types of CMC, (c–e) carbon powders of wood, coal and coconut, (f and g) MWNT and graphite fibers [109].

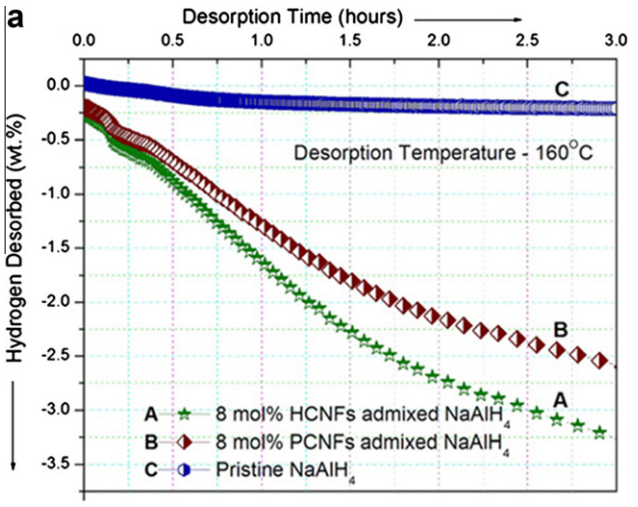

Fig. 27 Desorption kinetics, indicating desorption of hydrogen for helical CNFs admixed with $NaAlH_4$ (curve A), straight (planar) CNFs admixed with $NaAlH_4$ (curve B), and pristine $NaAlH_4$ (curve C) [110].

more electron emission sites and higher luminance, Fig. 25. They attributed this superior emission behaviour to the larger number of defect sites that exist in coiled carbon nanostructures, a phenomenon that is brought about by the non-linear morphology.

Gaseous ad/desorption behaviour

Hydrogen storage by carbon based materials has become an important area of research and the potential use of CMCs as a hydrogen storage material has been investigated. Furuya et al. [109] determined the absorption behaviour of as-grown CMCs (and those heat treated) and compared the results with those of multi-walled carbon nanotubes and activated carbons. They found that as-grown CMCs were capable of desorbing three to four times as much hydrogen as did multi-walled carbon nanotubes and active carbons, Fig. 26. When CMCs were heat treated at 850 °C there was a 20% increase in hydrogen adsorption. However when heat treated at 1000 °C there was a significant decrease in hydrogen adsorption. From activation energy calculations they concluded that desorption of hydrogen originates in the hydrocarbons formed on the as grown CMCs during the growth or cooling processes.

Raghubanshi et al. [110] considered the use of helical CNFs as a catalyst for improving the hydrogen desorption from $NaAlH_4$. They compared the desorption capabilities of pristine $NaAlH_4$, 8 mol% as-synthesized helical CNFs admixed with $NaAlH_4$ and 8 mol% as-synthesized planar (straight) CNFs admixed with $NaAlH_4$. They found that helical CNFs desorbed ~5× more hydrogen than pristine $NaAlH_4$ and ~30% more than planar CNFs, Fig. 27. Additionally they were able to show that for rehydrogenation studies pristine $NaAlH_4$ showed almost no re-adsorption whereas 8 mol% as-synthesized helical CNFs admixed with $NaAlH_4$ was capable of re-adsorbing 1.8 wt.% H_2. However it must be noted that purified helical CNFs showed lower re-adsorption behaviour as compared to the as-synthesized (unpurified) helical CNFs. Nevertheless helical materials, due to their unique structure, offer an interesting device to store hydrogen.

Polymer composites

Carbon materials with spring-like geometry are considered a fascinating carbon-based material that can be used as carbon fillers in reinforcement composites. The effectiveness of CMCs as a reinforcing material was investigated by Yoshimura et al. [111]. They showed that when CMCs were embedded in epoxy resin the mechanical properties of the composite could be altered. The Young's modulus as well as the tensile strength of the epoxy resins could be improved by the addition of just 2% CMCs. When compared to carbon fiber reinforced resins, the carbon micro-coil/epoxy resin showed better reinforcement capabilities. Yoshimura et al. attributed the enhanced abilities to the large specific surface area of the spring-shaped CMCs. They also suggested that the CMCs tended to extend with the polymer matrix and break only when an excessive load was applied. In contrast carbon fibers can be pulled out of the matrix due to the lack of interfacial adhesion.

In another study, Yoshimura et al. [112] considered the electrical properties of these composites and the effect that tensile and compressive strains have on the electrical resistivity. At low volume fractions (2% carbon content) CMC/silicon-rubber, CNF/silicon-rubber and carbon black/silicon-rubber all showed similar resistive behaviour. However as the volume fraction was increased (6%) there was dramatic decrease in resistivity for the CMC/silicon-rubber (100 Ω cm at 10% carbon content) and carbon nano-fiber/silicon-rubber composites, which was not observed for a carbon black/silicon-rubber composite. A significant decrease in resistivity was only seen after 15–25% carbon content. When exposed to a compressive or tensile strain, the resistivity of the CMC/silicon rubber composites increased considerably, whereas the carbon nano-fiber/silicon-rubber and carbon black/silicon-rubber composites

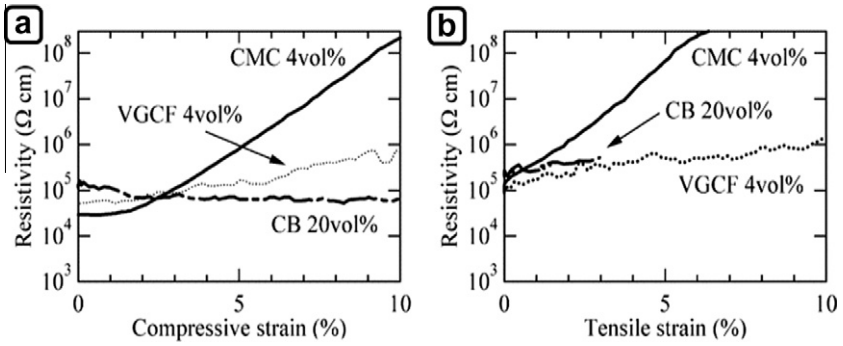

Fig. 28 Effect of strain on resistivity: (a) compressive strain, (b) tensile strain [112].

showed only slight changes, indicating that CMCs show greater sensitivity to strain, Fig. 28. They attributed this increase in resistivity to a change in the geometric structure of the CMCs upon strain.

Chen et al. [113] were able to show that tactile sensor elements of a very small size ($80 \times 80 \times 80\ \mu m^3$), composed of CMCs in polysilicone were capable of showing a very high sensitivity of 0.3 mgf. Additionally they found that tactile sensors incorporating carbon micro-coils had better discrimination abilities when compared to conventional sensors, making CMCs novel tactile sensors.

Katsuno et al. [114] showed that for CMC/silicone-rubber composites, the CMC content (%) affected various electrical properties viz. impedance, resistance and capacitance. The percolation paths (the critical transition which separates the dielectric state from the conductive one) were observed at 3% CMC content. Above the percolation threshold, the resistance decreased while the capacitance increased, providing insight into possible reasons as to why sensor size and carbon content affect electrical signals. Park et al. [115] compared the electromagnetic properties of straight single/multi-walled CNTs with that of coiled CNTs in polymer composites (reactive ethylene ter-polymer, constituted from polyethylene, polarmethyl-methacrylate and an epoxide). They found that the coiled or helical structure affected the electromagnetic properties of the polymer composite. Polymer composites with coiled carbon nanotubes showed a higher conductivity (and dielectric permittivity; two times larger than that obtained for straight tube composites) as well as enhanced electromagnetic interference shielding efficiency. They postulated that the increased conductivity related to the increased number of parallel resistors and capacitors due to the coiled morphology, which also makes available several alternative electrical conduction paths. Motojima et al. [116] considered the use of carbon micro-coil/polymethylmethacrylate (PMMA) composites for the absorption of electromagnetic waves in the high GHz region. The motivation for micro-coil use was intiated from studies conducted by Varadan et al. [117] who showed that conductive chiral (helical) polymers possessed excellent absorption properties. When Motojima et al. [116] compared the absorbtivity of PMMA (without CMCs), ferrite powder and carbon powder to that of a CMC/PMMA composite, they found that only the CMC/PMMA composite could absorb in the high GHz region. It was observed that the PMMA/CMC composite strongly absorbed electromagnetic waves with different absorption bands; greater than −30 dB at 81, 91 and 102 GHz. However at higher CMC content (5–10 wt.%) there was a decrease in the absorbtivity, probably due to increased electrical conductivity. Zhao et al. [118] considered the microwave absorption properties of CNC/paraffin wax composites and compared the composites with CMC composites. They found that composites incorporated with CNCs showed enhanced microwave absorption capabilities (90% absorption at 8.9–18 GHz) as compared to CMC composites. Wang et al. [82] showed that the electro-chemical properties (especially specific capacitance) could be determined from cyclic voltammetry and galvanostatic charging/discharging experiments. They prepared their electrodes as pellets by pressing together a mixture of CNCs (95%) and polytetraflouroethylene (5%). It was observed that the specific capacitance was ~ 40 F/g, which is three times higher than that of carbon micro-coils and six times higher than CNFs. They associated this remarkable observation with the open mesopores formed from the interconnected network and coiled (nano) structure.

Greenshileds et al. [119] showed that there is a noticeable difference in the vapour sensing capabilities of polyvinyl alcohol (PVA) composites incorporating multi-walled CNTs (MWCNTs/PVA), nitrogen-doped CNTs (N-MWCNTs/PVA) and coiled CNFs (CCNFs/PVA). It was observed that CCNF/PVA composites while ineffective for the detection of ethanol vapour, showed better performance and detection capabilities for methanol and toluene vapours (when compared to MWCNTs/PVA and N-MWCNTs/PVA composites). This study demonstrated that the three carbon nanostructure based composites (viz. MWCNTs/PVA, N-MWCNTs/PVA and CCNFs/PVA) show different responses when exposed to ethanol, methanol or toluene, and that, CCNFs are a unique and alternative material for incorporation in sensor devices.

Metalized carbon composites

Motojima et al. [120] showed that the properties of CMCs could be altered by vapour phase metallization to give SiC, TiC and ZrC. These novel metal carbides are potential candidates for use as conductive fillers, reinforcing fibers, electromagnetic shielding/absorber materials etc. For TiC (made from CMCs) it was observed that as the ratio of Ti/C was increased there was a corresponding decrease in the bulk resistivity of the materials. Furthermore, they found that when compared to TiC micro-tubes, TiC micro-coils did not attenuate the irradiated EM wave. In a later study Motojima et al. [121] observed that carbon micro-coils could act as a template for the selective preparation of TiO_2 micro-coils (polycrystal-

line anatase phase). This possibility of using carbon coils as a substrate was further extended by Bi et al. [122] who showed that the electromagnetic properties of carbon coils could be altered by coating them with Ni and P, thereby enhancing the microwave absorption ability of carbon coil composites. Perfect microwave absorbers can be obtained by optimizing the permittivity and permeability of a material, which is related to the magnetic and dielectric properties; these properties have also been investigated for coated and uncoated carbon micro-coils. Bi et al. [122] found that coated carbon micro-coils showed distinct variability when compared to uncoated carbon micro-coils. Their results indicated that by coating carbon micro-coils with Ni and P, they could control the magnetic and dielectric losses, thereby substantially increasing the electromagnetic energy dissipation. The effectiveness of carbon coils could be optimized by using specific materials that were capable of further modifying the magnetic and dielectric properties of the material. Recently Zhang et al. [123] showed that nano-coiled and micro-coiled CNFs could act as promising catalyst supports, offering superior electrooxidation of methanol when compared to a commercial carbon black. Pt particles supported on CMCs showed the highest electrocatalytic activity, with a fourfold enhancement when compared to that of Pt supported on carbon black. They were also able to deduce, from cyclic voltammetry, that CMCs and CNCs allowed for the Pt (110) crystallite phase to predominate, whereas carbon black allowed for the Pt (111) crystallite phase to predominate. They attributed the enhanced activity and selectivity (Pt phases) to the unique helical structure and composition of the carbon supports.

Biological applications

Motojima et al. [94] reported that CMCs have the ability to inhibit the breeding of keloid fibroblast, i.e., cancer cells associated with leukaemia of the uterus. This was motivated in part by studies conducted by Komura who observed that CMCs generated hydroxyl radicals in aqueous solution when exposed to ultrasound, and could be used for sonodynamic cancer treatments. When CMCs were added to skin cells (Pam 212) and collagen (mRNA), skin cell formation was promoted 1.6 times, whereas collagen formation increased 1.14 times (versus controls without CMCs). Currently CMCs have been commercialised as an additive in the cosmetic industry due to its collagen generating capabilities [124].

Summary

Carbon materials with helical morphology are considered in some cases to be superior alternatives to other linear carbon nanomaterials, a relationship that is said to be associated with the shape of the carbon material. However it must be noted that when one considers the electrical conductivity, field emission or the ad/desorption capabilities of helical carbon nanomaterials, their performance may be due to specific chemical and physical properties associated with the surface of the carbon helix rather than to the absolute structure of the material (coil, spring or helix) [109,110]. If helical carbon nanomaterials are compared to other non-helical carbon materials with a similar amorphous nature and content, there should be similar performances of the materials under investigation (this still needs to be assessed). Other than the mechanical behaviour of helical carbon nanomaterials, other properties associated with helicity require further investigation to ascertain whether helicity determines a property or if it is the fine structure of the material that is the determining factor.

Conclusion

The unique 3D morphology and associated properties of helical CNTs and CNFs has led many researchers to consider their use in various nano-technology applications. While there have been numerous synthetic procedures described in the literature to make helical carbon materials, absolute control over the coil morphology and yield still remains a challenge. However, it is expected that a better understanding of the growth mechanisms would ultimately aid in the design of improved systems, for the selective synthesis of helical materials in high yield. The unique electrical, mechanical, chemical and absorbance properties of carbon materials with helical morphology make them an ideal component for incorporation in numerous technological devices.

Acknowledgements

Financial support from the University of the Witwatersrand and the DST/NRF Centre of Excellence in Strong Materials is gratefully acknowledged.

References

[1] Coville NJ, Mhlanga SD, Nxumalo ED, Shaikjee A. A review of shaped carbon nanomaterials. S Afr J Sci 2011;107 [art. #418, 15 pages; doi:10.4102/sajs.v107i3/4.418].
[2] Zhang M, Li J. Carbon nanotube in different shapes. Mater Today 2009;12:12–8.
[3] Qi X, Qin C, Zhong W, Au C, Ye X, Du Y. Large-scale synthesis of carbon nanomaterials by catalytic chemical vapor deposition: a review of the effects of synthesis parameters and magnetic properties. Materials 2010;3:4142–74.
[4] Kathyayini H, Nagaraju N, Fonseca A, Nagy JB. Catalytic activity of Fe, Co and Fe/Co supported on Ca and Mg oxides, hydroxides and carbonates in the synthesis of carbon nanotubes. J Mol Catal A: Chem 2004;223:129–36.
[5] Dupuis A-C. The catalyst in the CCVD of carbon nanotubes-a review. Prog Mater Sci 2005;50:929–61.
[6] Dresselhaus MS, Dressalhaus G, Eklund PC. Science of fullerenes and carbon nanotubes. New York: Academic Press; 1996.
[7] Dresselhaus MS, Dresselhaus G, Avouris Ph (Eds). In: Carbon nanotubes: synthesis, structure, properties, and applications. Berlin: Springer-Verlag; 2001. p. 12–51.
[8] Ming J-H, Lin W-C. Unprecedented re-growth of carbon nanotubes on in situ re-activated catalyst. Nanotechnology 2009;20:0256081–85.
[9] Geim A K, Novoselov K S. The rise of graphene. Nat Mater 2007;6:183–91.
[10] Tsakadze ZL, Levchenko I, Ostrikov K, Xu S. Plasma-assisted self-organized growth of uniform carbon nanocone arrays. Carbon 2007;45:2022–30.
[11] Fejes D, Hernádi K. A review of the properties and CVD synthesis of coiled carbon nanotubes. Materials 2010;3:2618–42.

[12] Davis WR, Slawson RJ, Rigby GR. An unusual form of carbon. Nature 1953;171:756.
[13] Baker RTK, Gadsby GR, Thomas RB, Waite RJ. The production and properties of filamentous carbon. Carbon 1975;13:211–4.
[14] Qin Y, Zhang Z, Cui Z. Helical carbon nanofibers with a symmetric growth mode. Carbon 2004;42:1917–22.
[15] Ball P. Shapes: nature's patterns. New York: Oxford University Press; 2009, p. 1–32.
[16] Collins JA, Busby HR, Staab GH. Mechanical design of machine elements and machines. 2nd ed. New York: Wiley; 2009 [chapter 14].
[17] Korgel A. Nanosprings take shape. Mater Sci 2005;309:1683–4.
[18] Kane JW, Sternheim MM. Physics. 3rd ed. New York: J. Wiley; 1998 [chapter 16–20].
[19] Lau KT, Lu M, Hui D. Coiled carbon nanotubes: synthesis and their potential applications in advanced composite structures. Composites 2006;B37:437–48.
[20] Rodriguez NM, Chambers A, Terry R, Baker K. Catalytic engineering of carbon nanostructures. Langmuir 1995;11:3862–6.
[21] Dunlap BI. Connecting carbon tubules. Phys Rev 1992;B46:1933–6.
[22] Ihara S, Itoh S. Helically coiled and toroidal cage forms of graphitic carbon. Carbon 1995;33:931–9.
[23] Ihara S, Itoh S, Kitakami J-I. Toroidal forms of graphitic carbon. Phys Rev 1993;B47:12908–11.
[24] Fonseca A, Hernadi K, Nagy JB, Lambin Ph, Lucas A. A model structure of perfectly graphitizable coiled carbon nanotubes. Carbon 1995;33:1759–75.
[25] Biró LP, Mark GI, Lambin P. Regularly coiled carbon nanotubes. IEEE Trans Nanotechnol 2003;2:362–7.
[26] Dunlap BI. Relating carbon tubules. Phys Rev 1994;B49:5643–50.
[27] Setton R, Setton N. Carbon nanotubes: III. Toroidal structures and limits of a model for the construction of helical and s-shaped nanotubes. Carbon 1997;35:497–505.
[28] Liu LZ, Gao HL, Zhao JJ. Superelasticity of carbon nanocoils from atomistic quantum simulations. Nanoscale Res Lett 2010;5:478–83.
[29] Lu M, Li HL, Lau KT. Formation and growth mechanism of dissimilar coiled carbon nanotubes by reduced-pressure catalytic chemical vapor deposition. J Phys Chem B 2004;108:6186–92.
[30] Ramachandran CN, Sathyamurthy N. Introducing a twist in carbon nanotubes. Curr Sci 2006;91:1503–5.
[31] Amelinckx S, Zhang XB, Bernaerts D, Zhang XF, Ivanov V, Nagy JB. A formation mechanism for catalytically grown helix-shaped graphite nanotubes. Science 1994;265:635–9.
[32] Zhang L, Zhu YB, Ge CL, Wei C, Wang QL. The synthesis of carbon coils using catalyst arc discharge in an acetylene atmosphere. Solid State Commun 2007;142:541–4.
[33] Bandaru PR, Daraio C, Yang K, Rao AM. A plausible mechanism for the evolution of helical forms in nanostructure growth. J Appl Phys 2007;101:0943071–74.
[34] Liu W-C, Lin H-K, Chen Y-L, Lee C-Y, Chiu H-T. Growth of carbon nanocoils from K and Ag cooperative bicatalyst assisted thermal decomposition of acetylene. ACS Nano 2010;4:4149–57.
[35] Zhang Q, Yu L, Cui Z. Effects of the size of nano-copper catalysts and reaction temperature on the morphology of carbon fibers. Mater Res Bull 2008;43:735–42.
[36] Hokushin S, Pan L, Nakayama Y. Diameter control of carbon nanocoils by the catalyst of organic metals. Jpn J Appl Phys 2007;46:, 5383–5385.
[37] Tang N, Wen J, Zhang Y, Liu F, Lin K, Du Y. Helical carbon nanotubes: catalytic particle size-dependent growth and magnetic properties. ACS Nano 2010;4:241–50.
[38] Du F, Liu J, Guo Z. Shape controlled synthesis of Cu_2 O and its catalytic application to synthesize amorphous carbon nanofibers. Mater Res Bull 2009;44:25–9.
[39] Bai JB. Growth of nanotube/nanofibre coils by CVD on an alumina substrate. Mater Lett 2003;57:2629–33.
[40] Zhou X, Cui G, Zhi L, Zhang S. Large-area helical carbon microcoils with super hydrophobicity over a wide range of pH values. New Carbon Materials 2007;22:1–6.
[41] Motojima S, Kawaguchi M, Nozaki K, Iwanaga H. Preparation of coiled carbon fibers by catalytic pyrolysis of acetylene and its morphology and extension characteristics. Carbon 1991;29:379–85.
[42] Kawaguchi M, Nozaki K, Motojima S, Iwanaga H. A growth mechanism of regularly coiled carbon fibers through acetylene pyrolysis, J. Cryst Growth 1992;118:309–13.
[43] Chen X, Motojima S, Iwanaga H. Vapor phase preparation of super-elastic carbon microcoils. J Cryst Growth 2002;237–239:1931–6.
[44] Chen X, Motojima S. Growth of carbon micro-coils by pre-pyrolysis of propane. J Mater Sci 1999;34:3581–5.
[45] Yong Z, Fang L, Zhi-hua Z. Synthesis of heterostructured helical carbon nanotubes by iron-catalyzed ethanol decomposition. Micron 2011;42(6):547–52.
[46] Pan L, Zhang M, Nakayama Y. Growth mechanism of carbon nanocoils. J Appl Phys 2002;91:10058–61.
[47] Cheng J-B, Du J-H, Bai S. Growth mechanism of carbon microcoils with changing fiber cross-section shape. New Carbon Mater 2009;24:354–8.
[48] Yang S, Chen X, Motojima S. Vapor-phase formation of single-helix carbon microcoils by using WS2 catalyst and the morphologies. J Mater Sci 2004;39:2727–30.
[49] Xia JH, Jiang X, Jia CL, Dong C. Hexahedral nanocementites catalyzing the growth of carbon nanohelices. Appl Phys Lett 2008;92:0631211–13.
[50] Li D-W, Pan L-J, Liu D-P, Yu N-S. Relationship between geometric structures of catalyst particles and growth of carbon nanocoils. Chem Vap Depos 2010;16:166–9.
[51] Qin Y, Zhang Q, Cui Z. Effect of synthesis method of nanocopper catalysts on the morphologies of carbon nanofibers prepared by catalytic decomposition of acetylene. J Catal 2004;223:389–94.
[52] Shaikjee A, Franklyn PJ, Coville NJ. The use of transmission electron microscopy tomography to correlate copper catalyst particle morphology with carbon fiber morphology. Carbon 2011;49(9):2950–9.
[53] In-Hwang W, Yanagida H, Motojima S. Vapor growth of carbon micro-coils by the Ni catalyzed pyrolysis of acetylene using rotating substrate. Mater Lett 2000;43:11–4.
[54] AuBuchon JF, Chen L-H, Gapin AL, Kim D-W, Daraio C, Jin S. Multiple sharp bendings of carbon nanotubes during growth to produce zigzag morphology. Nano Lett 2004;4:1781–4.
[55] Joselevich E. Self-organised growth of complex nanotube patterns on crystal surfaces. Nano Res. 2009;2:743–54.
[56] Kyotani M, Matsushita S, Nagai T, Matsui Y, Shimomura M, Kaito A, Akagi K. Helical carbon and graphitic films prepared from iodine-doped helical polyacetylene film using morphology-retaining carbonization. J Am Chem Soc 2008;130:10880–1.
[57] Goh M, Matsushita T, Satake H, Kyotani M, Akagi K. Macroscopically aligned helical polyacetylene synthesized in magnetically orientated chiral nematic liquid crystal field. Macromolecules 2010;43:5943–8.
[58] Szabo A, Fonseca A, Nagy JB, Lambin Ph, Biro LP. Structural origin of coiling in coiled carbon nanotubes. Carbon 2005;43:1628–33.
[59] Qi X, Yang Y, Zhong W, Deng Y, Au C, Du Y. Large-scale synthesis, characterization and microwave absorption

properties of carbon nanotubes of different helicities. J Solid State Chem 2009;182:2691–7.
[60] Qi X, Zhong W, Deng Y, Au C, Du Y. Synthesis of helical carbon nanotubes, worm-like carbon nanotubes and nanocoils at 450 °C and their magnetic properties. Carbon 2010;48:365–76.
[61] Daraio C, Nesterenko VF, Jin S. Impact response by a foamlike forest of coiled carbon nanotubes. J Appl Phys 2006;100:0643091–94.
[62] Kong Q, Zhang J. Synthesis of straight and helical carbon nanotubes from catalytic pyrolysis of polyethylene. Polym Degrad Stab 2007;92:2005–10.
[63] Wang W, Yang K, Gaillard J, Bandaru PR, Rao AM. Rational synthesis of helically coiled carbon nanowires and nanotubes through the use of tin and indium catalysts. Adv Mater 2008;20:179–82.
[64] Hernadi K, Thiên-Nga L, Forró L. Growth and microstructure of catalytically produced coiled carbon nanotubes. J Phys Chem B 2001;105:12464–8.
[65] Fejes D, Németh Z, Hernádi K. CVD synthesis of spiral carbon nanotubes over asymmetric catalytic particles. React Kinet Catal Lett 2009;96:397–404.
[66] Cheng J, Zhang X, Tu J, Tao X, Ye Y, Liu F. Catalytic chemical vapor deposition synthesis of helical carbon nanotubes and triple helices carbon nanostructure. Mater Chem Phys 2006;95:12–5.
[67] Zhang Q, Zhao M-Q, Tang D-M, Li F, Huang J-Q, Liu B, Zhu W-C, Zhang Y-H, Wei F. Carbon-nanotube-array double helices. Angew Chem 2010;122:3724–7.
[68] Somanathan T, Pandurangan A. Helical multiwalled carbon nanotubes (h-MWCNTs) synthesized by catalytic chemical vapor deposition. New Carbon Mater 2010;25:175–80.
[69] Zhong D-Y, Liu S, Wang EG. Patterned growth of coiled carbon nanotubes by a template-assisted technique. Appl Phys Lett 2003;83:4423–5.
[70] Sevilla M, Fuertes AB. Easy synthesis of graphitic carbon nanocoils from saccharides. Mater Chem Phys 2009;113:208–14.
[71] Ren X, Zhang H, Cui Z. Acetylene decomposition to helical carbon nanofibers over supported copper catalysts. Mater Res Bull 2007;42:2202–10.
[72] Yu L, Qin Y, Cui Z. Synthesis of coiled carbon nanofibers by Cu-Ni alloy nanoparticles catalyzed decomposition of acetylene at low temperature of 241 °C. Mater Lett 2005;59:459–62.
[73] Shaikjee A, Coville NJ. The effect of copper catalyst reducibility on low temperature carbon fiber synthesis. Mater Chem Phys 2011;125:899–907.
[74] Jian X, Jiang M, Zhou Z, Yang M, Lu J, Hu S, Wang Y, Hui D. Preparation of high purity helical carbon nanofibers by the catalytic decomposition of acetylene and their growth mechanism. Carbon 2010;48:4535–41.
[75] Fukuda T, Watabe N, Whitby R, Maekawa T. Creation of carbon onions and coils at low temperature in near-critical benzene irradiated with an ultraviolet laser. Nanotechnology 2007;18:4156041–46.
[76] Chesnokov VV, Zaikovskii VI, Buyanov RA. Symmetric twisted carbon filaments formed from butadiene-1,3 on Ni–Cu/MgO-catalyst: growth regularities and mechanism. J Mol Catal A: Chem 2000;158:267–70.
[77] Tang N, Kuo W, Jeng C, Wang L, Lin K, Du Y. Coil-in-coil carbon nanocoils: 11 gram-scale synthesis, single nanocoil electrical properties, and electrical contact improvement. ACS Nano 2010;4:781–8.
[78] Jia M, Zhang Y. Study on the synthesis of carbon fibers and CNF using potassium iodide catalyst. Mater Lett 2009;63:2111–4.
[79] Qin Y, Zhang Y, Sun X. Synthesis of helical and straight carbon nanofibers by chemical vapor deposition using alkali chloride catalysts. Microchim Acta 2009;164:425–30.
[80] Ivanov V, Nagy JB, Lambin Ph, Lucas A, Zhang XB, Zhang XF, Bernaerts D, Van Tendeloo G, Amelinckx S, van Landuyt J. The study of carbon nanotubules produced by catalytic method. Chem Phys Lett 1994;223:329–35.
[81] Motojima S, Kagiya S, Iwanaga H. Vapour-phase formation of micro-coiled carbon fibres using Ni catalyst and PH_3 impurity. Mater Sci Eng 1995;B34:47–52.
[82] Wang L, Li C, Gu F, Zhang C. Facile flame synthesis and electrochemical properties of carbon nanocoils. J Alloys Compd 2009;473:351–5.
[83] Lu W-X, Sui Z-J, Zhou J-H, Li P, Chen D, Zhou X-G. Kinetically controlled synthesis of carbon nanofibers with different morphologies by catalytic CO disproportionation over iron catalyst. Chem Eng Sci 2010;65:193–200.
[84] Yang S, Chen X, Katsuno T, Motojima S. Controllable synthesis of carbon microcoils/nanocoils by catalysts supported on ceramics using catalyzed chemical vapor deposition. Mater Res Bull 2007;42:465–73.
[85] Yang S, Ozeka I, Chen X, Katsuno T, Motojima S. Preparation of single-helix carbon microcoils by catalytic CVD process. Thin Solid Films 2007;516:718–21.
[86] Hanus MJ, Harris AT. Synthesis of twisted carbon fibers comprised of four intertwined helical strands. Carbon 2010;48:2989–99.
[87] Bi H, Kou KC, Ostrikov K, Yan LK, Zhang JQ. Unconventional Ni–P alloy-catalyzed CVD of carbon coil-like micro- and nano-structures. Mater Chem Phys 2009;116:442–8.
[88] Yang S, Chen X, Kikuchi N, Motojima S. Catalytic effects of various metal carbides and Ti compounds for the growth of carbon nanocoils (CNSs). Mater Lett 2008;62:1462–5.
[89] Yang S, Zao H, Chen X. Vapor growth of novel carbon submicro-fibers with a tile-like form and carbon nanofibers with zigzag form. Vacuum 2006;81:385–8.
[90] Chang N-K, Chang S-H. High-yield synthesis of carbon nanocoils on stainless steel. Carbon 2008;46:1091–109.
[91] Bi H, Kou K-C, Ostrikov K, Wang Z-C. High-yield atmospheric-pressure CVD of highly-uniform carbon nanocoils using Co–P catalyst nanoparticles prepared by electroless plating. J Alloys Compd 2009;484:860–3.
[92] Liu J, Zhang X, Zhang Y, Chen X, Zhu J. Nano-sized double helices and braids: interesting carbon nanostructures. Mater Res Bull 2003;38:261–7.
[93] Banerjee D, Mukherjee S, Chattopadhyay KK. Synthesis of carbon nanowalls by DC-PECVD on different substrates and study of its field emission properties. Appl Surf Sci 2011;257:3717–22.
[94] Motojima S. Development of ceramic microcoils with 3D-herical/spiral structures. J Cer Soc Jpn 2008;116:921–7.
[95] Wang J-S, Cui Y-H, Feng X-Q, Wang G-F, Qin Q-H. Surface effects on the elasticity of nanosprings. EPL 2010;92:160021–6.
[96] Chen X, Zhang S, Dikin DA, Ding W, Ruoff RS, Pan L, Nakayama Y. Mechanics of a carbon nanocoil. Nano Lett 2003;3:1299–304.
[97] Hayashida T, Pan L, Nakayama Y. Mechanical and electrical properties of carbon tubule nanocoils. Phys B (Amsterdam, Neth) 2002;323:352–3.
[98] Bi H, Kou KC, Ostrikov K, Zhang JQ, Wang ZC. Mechanical model and superelastic properties of carbon microcoils with circular cross-section. J Appl Phys 2009;106:023520.
[99] Poggi MA, Boyles JS, Bottomley LA, Mcfarland AW, Colton JS, Nguyen CV, Stevens RM, Lillehei PT. Measuring the compression of a carbon nanospring. Nano Lett 2004;4:1009–16.

[100] Chang NK, Chang SH. Determining mechanical properties of carbon microcoils using lateral force microscopy. IEEE Trans Nanotechnol 2008;7:197–201.
[101] Volodin A, Buntinx D, Ahlskog M, Fonseca A, Nagy JB, Van Heasendonck C. Coiled carbon nanotubes as self-sensing mechanical resonantors. Nano Lett 2004;4:1775–9.
[102] Kaneto K, Tsuruta M, Motojima S. Electrical properties of carbon micro coils. Syn Met 1999;103:2578–9.
[103] Chiu H-S, Lin P-I, Wu H-C, Hsieh W-H, Chen C-D, Chen Y-T. Electron hopping conduction in highly disordered carbon coils. Carbon 2009;47:1761–9.
[104] Liu C-J, Wu T-W, Hsu L-S, Su C-J, Wang C-C, Shieu F-S. Transport properties of spiral carbon nanofibers mats containing Pd metal clusters using Pd_2 $(dba)_3$ as catalyst. Carbon 2004;42:2635–40.
[105] Fujii M, Matsui M, Motojima S, Hishikawa Y. Magnetoresistance in carbon micro-coils obtained by chemical vapour deposition. Thin Solid Films 2002;409:78–81.
[106] Kato Y, Kojima T, Miwa H, Tsuda T, Yoshida T, Motojima S. Expanding and contracting motions of carbon micro-coils induced by alternating current. Jpn J Appl Phys 2006;45:2695–8.
[107] Zhang G, Jiang X, Wang E. Self-assembly of carbon nanohelices: characteristics and field electron emission properties. Appl Phys Lett 2004;84:2646–8.
[108] Zhang Z, He P, Sun Z, Feng T, Chen Y, Li H, Tay BK. Growth and field emission property of coiled carbon nanostructure using copper as catalyst. Appl Surf Sci 2010;256:4417–22.
[109] Furuya Y, Hashishin T, Iwanaga H, Motojima S, Hishikawa Y. Interaction of hydrogen with carbon coils at low temperature. Carbon 2004;42:331–5.
[110] Raghubanshi H, Hudson MSL, Srivastava ON. Synthesis of helical carbon nanofibers and its application in hydrogen desorption. Int J Hydrogen Energy 2011;36(7):4482–90.
[111] Yoshimura K, Nakano K, Miyake T, Hishikawa Y, Motojima S. Effectiveness of carbon microcoils as a reinforcing material for a polymer matrix. Carbon 2006;44:2833–8.
[112] Yoshimura K, Nakano K, Miyake T, Hishikawa Y, Kuzuya C, Katsuno T, et al. Effect of compressive and tensile strains on the electrical resistivity of carbon microcoil/silicone-rubber composites. Carbon 2007;45:1997–2003.
[113] Chen X, Yang S, Hasegawa M, Kawabe K, Motojima S. Tactile microsensor elements prepared from arrayed superelastic carbon microcoils. Appl Phys Lett 2005;87:0541011–13.
[114] Katsuno T, Chen X, Yang S, Motojima S, Homma M, Maeno T, et al. Observation and analysis of percolation behaviour in carbon microcoils/silicone-rubber composite sheets. Appl Phys Lett 2006;88:2321151–53.
[115] Park SH, Theilmann P, Yang K, Rao AM, Bandaru PR. The influence of coiled nanostructure on the enhancement of dielectric constants and electromagnetic shielding efficiency in polymer composites. Appl Phys Lett 2010;96:431151–3.
[116] Motojima S, Hoshiya S, Hishikawa Y. Electromagnetic wave absorption properties of carbon microcoils/PMMA composite beads in W bands. Carbon 2003;41:2653–9.
[117] Varadan VK, Varadan VV. Electromagnetic shielding and absorptive materials. USP 1990:4948922.
[118] Zhao D-L, Shen Z-M. Preparation and microwave absorption properties of carbon nanocoils. Mater Lett 2008;62:3704–6.
[119] Greenshileds MWCC, Hümmelgen IA, Messai AM, Shaikjee A, Mhlanga SD, van Otterlo WAL, et al. Composites of polyvinyl alcohol and carbon (coils, undoped and nitrogen doped multiwalled carbon nanotubes) as ethanol, methanol and toluene vapor sensors, Journal of Nanoscience and Nanotechnology (in press 2011).
[120] Motojima S, Yang S, Chen X, Iwanaga H. Preparation and properties of TiC micro-coils and micro-tubes by the vapour phase titanizing of carbon micro-coils. J Mater Sci 1999;34:5989–94.
[121] Motojima S, Suzuki T, Noda Y, Hiraga A, Iwanaga H, Hashishin T, et al. Preparation of TiO_2 microcoils from carbon microcoil templates using a sol–gel process. Chem Phys Lett 2003;378:111–6.
[122] Bi H, Kou K-C, Ostrikov K, Yan L-K, Wang Z-C. Microstructure and electromagnetic characteristics of Ni nanoparticles film coated carbon microcoils. J Alloys Compd 2009;478:796–800.
[123] Zhang L, Li F. Helical nanocoiled and microcoiled carbon fibers as effective catalyst supports for electrooxidation of methanol. Electrochim Acta 2010;55:6695–702.
[124] Chen X, Motojima S. Vapor phase preparation and some properties of carbon micro-coils (CMCs). KONA 2006;24:222–6.